Improvements to the Design of a Flexible Diaphragm for use in Pressure Wave Generators for Cryogenic Refrigeration Systems.

A thesis submitted in partial fulfilment of the

requirements for the Degree

of Master of Engineering

in the University of Canterbury

by Kent Hamilton

University of Canterbury

2013

Abstract

Low cost cryocoolers suitable for long term use in industrial environments are required for superconducting technologies to be competitive with copper based devices in real world applications. Industrial Research Limited is developing such cryocoolers, which use metal diaphragm based pressure wave generators to convert electrical energy to the gas volume displacement required. This project explores methods of increasing the volume displacement provided by the diaphragms while ensuring the components stay within the acceptable material limits.

Various alternative diaphragm shapes are tested against the currently used shape through finite element analysis. In addition to testing alternative diaphragm shapes, each shape's dimensions are optimised. It is concluded the currently used design can be improved by offsetting the piston rest position and slightly reducing the piston diameter.

A more detailed analysis is carried out of the bend radii created during fabrication of the diaphragm, and physical testing is performed to verify unexpected calculated stress concentrations. High stresses are observed, however it is concluded unmodelled material features have a large effect on the final stress distribution.

It is recommended advantageous shape changes calculated in the first part of the work be trialled to increase the efficiency of the cryocooler, and that investigation of the material behaviour during commissioning of the pressure wave generator be carried out to better understand the operational limits of the diaphragms.

Acknowledgements

I wish to thank:

Alan Caughley: For technical supervision and assistance in creating and working through concepts, as well as understanding the technology and application.

Keith Alexander: For academic supervision and assistance in identifying and assessing problems, as well as his advice on conducting effective research.

The workshop staff at both Industrial Research Limited Christchurch and the University of Canterbury: For their assistance in supplying and manufacturing the necessary components as well as providing advice and equipment to help accomplish the project goals.

Industrial Research Limited: For funding and support.

Contents

1 Introduction

High Temperature Superconductor (HTS) based technology has the potential to greatly improve the efficiency of electric power generation, distribution, storage and use[1]. HTS cables and windings are able to support higher density current than presently used metal conductors, allowing equipment to be built smaller and lighter while maintaining the same power handling capability. In addition HTS cables have zero electrical resistance, greatly reducing the energy losses due to resistive heating.

HTS materials must be kept below 93 K for superconduction to occur, with additional cooling further increasing the material's current capacity. The majority of HTS devices presently in development operate at the boiling point of nitrogen, 77 K, so the required cooling may be attained by immersing the device in a liquid nitrogen bath. As the liquid evaporates at room temperature any bath containing operating HTS equipment must be continuously topped up to ensure superconductivity persists. The quantity of liquid nitrogen increases further with machines which operate with alternating current as inductive losses produce additional heat.

Liquid nitrogen is presently commercially produced in large quantities for a variety of applications. Institutions developing HTS equipment generally buy the liquid and store it in dewars, ordering additional liquid when supplies are low. For HTS devices to be commercially viable they must be able to run unattended, and so should include refrigeration equipment rather than relying on frequent liquid nitrogen refills.

The refrigerator will be required continuously, must be economic at the smaller scale, and must be constructed of equipment suitable for deployment in industrial and/or low maintenance environments.

Industrial Research Limited (IRL) began cryogenic refrigeration research in 2005[2], after the United States Department of Energy highlighted cryogenic cooling as an important enabling technology in need of development in anticipation of emerging HTS technologies. IRL has since produced several functional examples of industrial cryocoolers utilising a novel diaphragm pressure wave generator (PWG) based design.

This thesis describes efforts to increase the reliability and efficiency of the IRL cryocooler design by investigating potential changes to the design of flexible metal diaphragms used within the PWG. The presently used diaphragms have not been optimised for mechanical efficiency and fail in a manner not predicted by the original design. Additionally the present design has been shown to be capable of greater efficiency when run in conditions beyond the original design specification[3], i.e. at a lower factor of safety. The planned outcome was the production of an improved diaphragm, and a greater understanding of the existing diaphragms' behaviour. To accomplish these goals, modelling and optimisation of the existing diaphragm and alternative concept designs was performed using finite element (FE) analysis software, and the validity of the FE modelling checked by comparing the calculated stresses with those measured in an in service diaphragm.

2 Background

2.1 Stirling Engine Flexible Diaphragm Development

The IRL concept of using flexible metal diaphragms to produce low maintenance reciprocating equipment is similar to thermal mechanical generators (TMG) developed by Cooke-Yarborough in the second half of last century[4]. The six main features are shown in figure 2.1. These are the hot cavity, cold cavity, heat source, reciprocating displacer, regenerator and the diaphragm. The housing, diaphragm and regenerator form a sealed chamber filled with helium gas in which the displacer sits. The TMG is similar to free piston Stirling engine that converts heat from the heat source into electricity using the following cycle[5]:

1. Expansion of heated gas deflects the diaphragm upward, doing work.
2. The displacer is moved into the hot cavity, pumping gas from the hot cavity into the cold cavity. As the gas is displaced it passes the regenerator which collects some of the heat.
3. The low pressure of the cool gas in the cold cavity deflects the diaphragm downward. Momentum causes the diaphragm deflection to be greater than is required to equalise the pressure, resulting in compression of the gas and sinking of the heat through the diaphragm to the ambient temperature.
4. The displacer moves upward, collapsing the cold cavity and moving the cold gas to the hot cavity. Heat is transferred to the gas as it passes the regenerator, and additional heat is introduced to the system by the heat source. Heating of the gas causes the gas expansion in step 1.

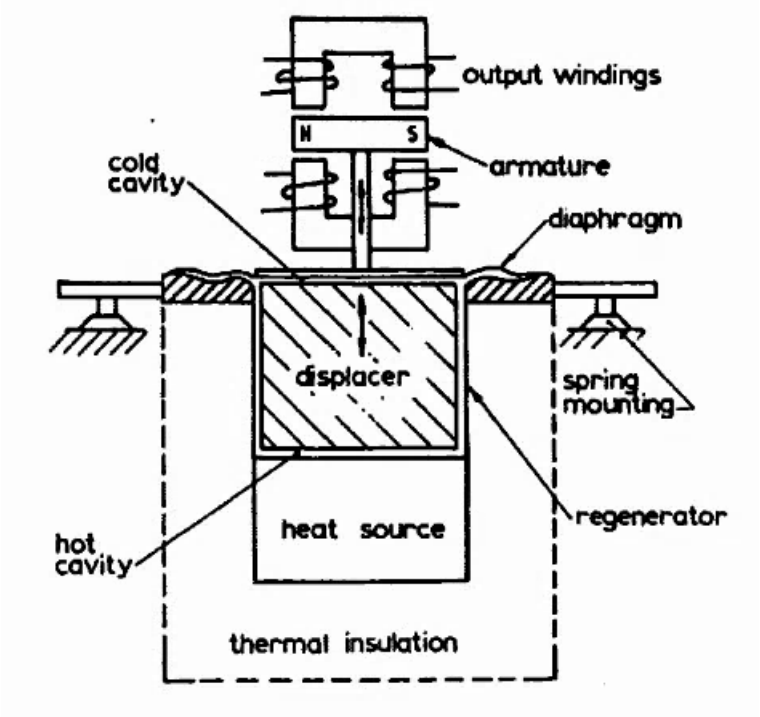

Figure 2.1: Cooke Yarborough thermal mechanical generator schematic showing main components, from [5].

Electricity is generated from the movement of the diaphragm via a linear generator as shown at the top of the figure, not shown in the figure is a stiff spring which centres the displacer. The oscillation of the displacer is the natural frequency of the spring mass system that is the stiff spring and displacer. This causes the displacer movement to be 90 degrees out of phase with the diaphragm movement as described above.

The Cooke-Yarborough generators were designed for installation in lighthouses or other remote locations where fuel and maintenance could not be frequently supplied, so needed to be able to reliably operate for extended periods of time while using as little fuel as possible, and were proven capable of operating for over ten years when powered by radio-isotope heat sources, while only requiring basic maintenance approximately once every three years.

The flexible metal diaphragm in Cooke-Yarborough's design enabled high efficiency and reliability of the TMG by being the seal between the ambient and working gas environments, rather than relying on sliding piston rings as is done in most heat engines. Eliminating sliding surfaces from the design prevented machine wear and removed the need for lubrication. The lack of friction also increased the machine's efficiency.

The diaphragm and other flexible components in the TMG were designed to remain below the fatigue limit of their respective materials at all times, meaning the generator could theoretically operate indefinitely as long as the heat source persists. To ensure these limits were not exceeded the diaphragm displacement is very small compared with the diaphragm radius. This is a constraint also present in the IRL PWG, as is the requirement for the diaphragm to be impermeable to helium, as both machines use helium as the working gas.

2.2 IRL Cryocooler Design

The PWG is the component of the system that manipulates the working gas; in the case of the IRL PWG this is a flexible metal diaphragm, a piston which oscillates the diaphragm, and the drivetrain that reciprocates the piston. The PWG is analogous to the linear motor in the example described in section 2.1. As the Stirling cycle is reversible, driving the working gas causes a temperature difference between the hot and cold cavities which can be used to create cryogenic cooling.

The IRL PWG is unique in that it separates a conventionally lubricated mechanical driven piston from the clean helium working gas with a flexible metal diaphragm, rather than sealing the working gas above the piston with lubricated piston rings as is common in conventional PWGs. The IRL arrangement eliminates the piston rings, preventing contamination of the helium by oil or other lubricants which would otherwise lower the machine's efficiency. As the piston and driving mechanism do not come in contact with the helium, conventional industrial components and lubrication can be used, resulting in a cheaper PWG which can be maintained using conventional industrial knowledge and equipment.

The helium working gas is kept at an average pressure of 2.5 MPa, and the diaphragm must contain this pressure at all times including when the PWG is idle. At the bottom end of the PWG is a second diaphragm which forms an air spring with the housing, also pressurised at 2.5 MPa. The gas spring balances the force of the working gas pressure at the top of the piston meaning the force from this pressure is not transferred to the piston drive mechanism. In combination with a 10:1 lever arrangement, this balanced force allows the PWG to be driven at 60 Hz with a conventional electric motor.

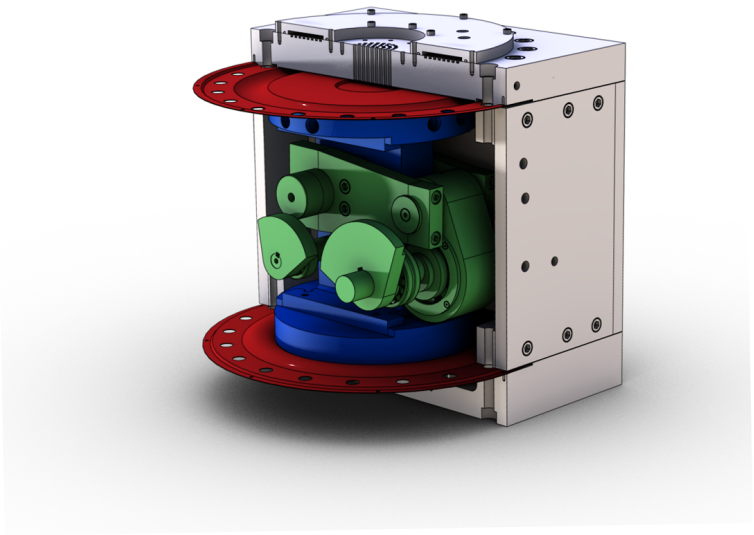

Figure 2.2: Cutaway diagram of an IRL pressure wave generator. The diaphragms are shown in red, the piston in blue, the piston driver in green, and the frame in grey. Connection points for the pulsetube can be seen in the top of the frame, above the upper diaphragm.

2.3 Other Flexible Diaphragm Prior Work

Flexible diaphragms are used in many situations where gas pumping or flexible seals are required. Recent advances in modelling the efficiency and stroke capacity of diaphragm shapes have been mainly in the field of microfluidics and the miniaturisation of microphones or speakers, where the components are made from silicon, have radii less than 10 mm, and are not required to operate under high differential pressure.

Corrugated diaphragms have excellent flexibility at large displacements[7], although the design exhibits greater stiffness at small displacements due to the corrugation sides having greater flexural rigidity tangentially, i.e. the stiffness of the diaphragm is increased by material that is not perpendicular to the displacement direction[6]. At greater deflections the tensile rigidity is more important, as more stretching and less bending is required from the diaphragm[7]. Additionally it was shown the number of corrugations has little effect on the diaphragm performance, with the depth of the corrugations resulting having a much greater effect.

The work of Nguyen et al[8] differs in that it considers the edge conditions, and shows displacement can be increased by simply supporting, rather than cantilevering, the edges of the diaphragm. This arrangement reduces the amount of diaphragm material subjected to bending.

Adolf Brendlin's work concentrates of improving the efficiency of flexible diaphragms for use in bellows where high pressure differences exist across the diaphragms[9]. Efficiency is gained by increasing the transverse stiffness of the interfaces while retaining the radial flexibility in the diaphragms. Bending stresses caused by corrugations inflating with the pressure are reduced while diaphragm deflection is maximised. Patents held by Brendlin are included as appendices A and B; the main concept behind these being mechanical support of the corrugations which face into the pressure vessel as shown in figure 2.3.

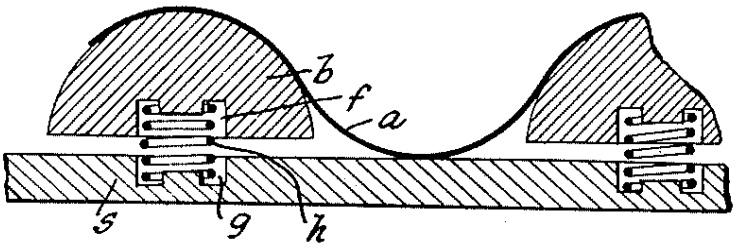

Figure 2.3: Example bellows support structure from Adolf Brendlin's patent (#2203859). In this cross-section view the diaphragm is marked a, and the support b. Items s, g, h and f make up a moving support structure to follow the deflection of the diaphragm during operation.

3 Presently used IRL Diaphragm Design

The presently used diaphragm design is 470 mm diameter flat plate with a cupped ring as shown in figure 3.1. This ring is unsupported when the PWG is operating, while the flat interior and exterior disks are supported by the piston and PWG frame respectively, as can be seen in figure 2.2. The central diaphragm indentation is for locating the piston, and the holes through the outer disk are for clamping bolts that secure the diaphragm as one wall of the working gas or gas spring pressure vessel.

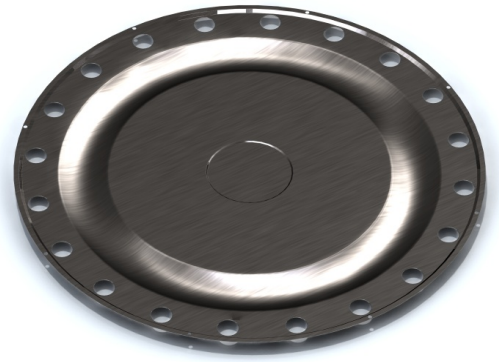

Figure 3.1: Computer generated image of the presently used diaphragm design including an indication of the brushed surface finish present in the failed diaphragm investigated in section 4.

The diaphragm is manufactured from 0.7 mm thick ferritic stainless steel (AISI 430) by spin forming or pressing. Several other diaphragm sizes exist as IRL is developing different capacity PWGs which have different displacement requirements, these additional sizes have the same shape, scaled up or down to fit the alternative PWGs.

3.1 Design Requirements

The primary function of the diaphragm is to transfer the mechanical work of the piston to the helium working gas contained in the pressure vessel. The diaphragm must also prevent degradation of the helium and keep the piston centred relative to the drive mechanism.

Helium degradation can be caused by contamination (i.e. material entering the pressure vessel) or pressure reduction (helium escaping the vessel).

The design requirements of this existing diaphragm are applicable to any diaphragm modification, and are that the diaphragm must:

- Transfer piston force to the working gas.
- Contain helium at pressure (25 Bar).
- Prevent contamination of the contained gas.
- Have a design life exceeding 40000 hours at an operating frequency of 60 Hz.
- Keep the piston aligned with the drive mechanism and PWG frame.

The expectations of an improved diaphragm are that in addition to the requirements listed above, the swept volume of the operating diaphragm is increased above that of the current diaphragm, while maintaining the 28% safety factor employed by the current design, and without increasing the radius. It is also desired that the diaphragm remains relatively flat so as not to increase the overall height of the PWG dramatically, and that the compression space reduces as much as possible during the compression cycle to minimise the amount of helium not used in the pressure wave cycle.

3.2 Previous Design Methods

The cupped shape of the existing unsupported diaphragm region mimics the shape shown in the Stirling engine work of Cooke-Yarborough and aims to be a compromise between the ideal flat plate for bending and the ideal tube for containing pressure. Several iterations of the shape were investigated, adjusting the depth of the indentation by manipulating the radius of the cup. These iterations were compared using finite element (FE) methods in the SolidWorks computer aided design suite. The Von-Mises stress distribution on the upper surface of the diaphragm when the piston is raised 1.5 mm as calculated in SolidWorks is shown in figure 3.2.

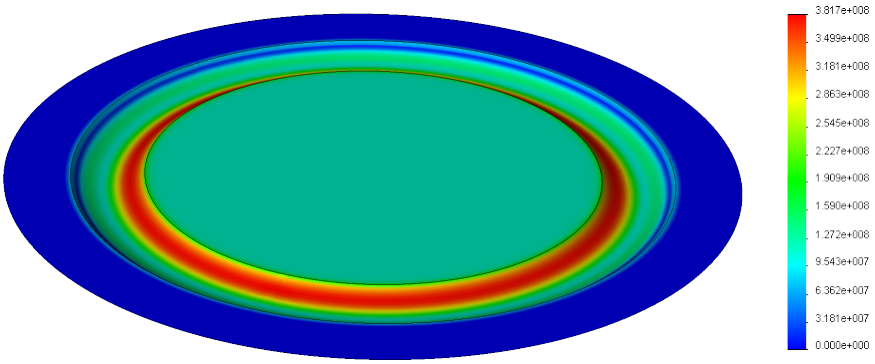

Figure 3.2: Von-Mises stress distribution at the upper surface of the diaphragm when a positive displacement of 1.5 mm is applied as calculated using the original IRL FE model created in SolidWorks.

The fatigue life of several potential materials was assessed by accelerated fatigue testing performed at IRL. AISI 430 stainless steel was found not to have failed after 1.0e8 cycles at an alternating stress amplitude of 450 MPa[4]. Increasing the stress to 580 MPa caused failures after as few as 2.5e6 cycles. The fatigue life of the material was taken to be 450 MPa, or 352 MPa with a 28% safety factor. Designs in which the maximum stress was calculated to remain below the fatigue life of the material were assumed to be capable of continuous operation exceeding the required design life.

3.3 Dimensions and Performance

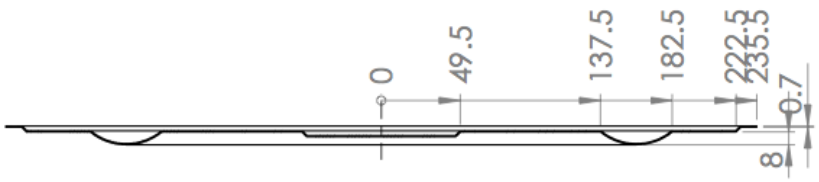

Figure 3.3: Dimensions of the presently used diaphragm in millimetres.

The specific dimensions of the diaphragm as designed are shown in figure 3.3. These dimensions do not take into account manufacturing features such as bend radii and membrane shapes created during pressing and were modelled as the dimensions of the lower face of the sheet. Manufacturing features are covered in greater detail in section 5.

IRL's PWG using this diaphragm has an overall efficiency of 72%. This figure is below the 78% reported of the Oxford style PWG; however installation of a higher efficiency motor in the IRL machine is expected to reduce this difference[4], making the present design comparable in performance while being more reliable with lower maintenance requirements.

In 2010 a higher displacement PWG was required for operation with a higher capacity pulse tube refrigerator. The PWG stroke was increased from ± 1.25 mm to ± 1.5 mm by changing only the crank throw. This resulted in an increase in the power output by more than the expected 20% as well as efficiency gains, but did reduce the safety factor of the diaphragm to 10% as calculated by the SolidWorks FE model. This greater than expected increase in efficiency highlighted diaphragm stroke capability as an area in which the PWG could be improved.

The diaphragms in the modified PWG were produced by spin forming and have thus far lasted over 7000 hours operation. However, several press formed diaphragms used in unmodified cryocoolers have failed near the interface between the flat central disk and the filleted edge. This is not the expected failure point as calculated in the FE models used during design of the diaphragm.

Fractures at the bend can be due to fretting caused by the piston edge sliding against the diaphragm. Early in development of the PWG such fractures occurred at around 10^7 cycles. An acetyl layer was then added between the piston and diaphragm and evidence of fretting no longer appears. Section 4 details investigation of the fracture. To improve understanding of diaphragm reliability this thesis aims to identify the cause of these fractures and design methods of reducing the probability of these and any other fractures in the diaphragm.

4 Fracture Analysis

A study of the fracture in an example diaphragm was carried out with the aim of better understanding the cause and development of the failure.

4.1 Visual Inspection

The failed diaphragm investigated is a 470 mm diaphragm pressed from AISI 430 stainless steel with a brushed finish. The fracture occurred approximately 1 mm outside the limit of the flat interior disk of the diaphragm as shown in figure 4.1. The fracture is a through crack approximately 10 mm long in the same direction as the brushed texture of the component.

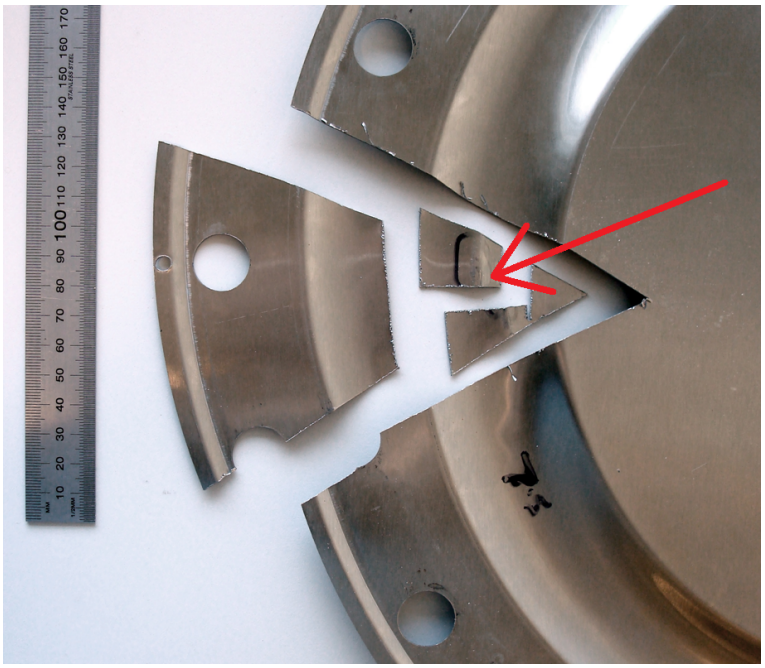

Figure 4.1: Failed diaphragm during sectioning for analysis. The through crack is at the position indicated by the arrow, tangential to the brushed surface finish and approximately 10 mm long.

Visual inspection shows no evidence of damage to the area around the crack, nor are there any non-axisymmetric features that would cause the failure to occur at this point, other than the brushed texture. This diaphragm was installed in a PWG with a PTFE disk between the diaphragm and piston, and there is no evidence of fretting at the failure point.

4.2 Sample Preparation

The diaphragm was cut so the fracture surface could be seen, and the exterior half prepared for microscopy and microhardness testing. The sample was set in a resin plug, ground to a 600 grit finish, polished to 1 μm and finally polished to a 0.06 μm finish with silica slurry. To accentuate the grain boundaries the resulting surface was etched using glyceregia. The interior side was inspected with a scanning electron microscope (SEM), the sample was cleaned and mounted in a small vice and placed on the microscope stage. Coating was not required as the expected material (430 stainless steel) is conductive.

4.3 Material Identification

Optical microscope inspection aimed to check the composition of the component material to ensure it is the expected AISI 430 ferritic stainless steel, and of what quality. Additionally hardness testing was done to further verify the material.

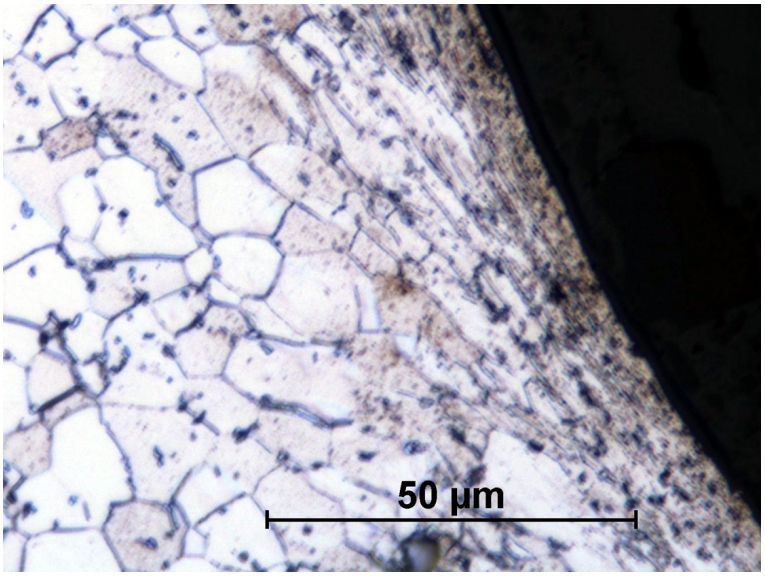

Figure 4.2: Optical microscope image of a cross-section of the diaphragm near the failure position. The material appearance matches that expected of 430 Stainless steel. Elongated grains can be seen near the material surface.

An optical microscope image is presented in figure 4.2, and the results of hardness testing in table 1. The microscope images show grain structure consistent with that of ferritic stainless steel, and the hardness measured is within the 150-195 HV range expected of AISI 430[10]. The material hardness is greater toward the top surface, where the grains are elongated as shown in figure 4.2. The higher hardness and elongated grains at the top surface may have some effect on its fatigue life as they indicate there are residual compressive strains from the production of the stock metal sheet. The higher hardness also indicates the No internal defects were observed, however the sectioned faces show the material close to the fracture location, rather than the fracture surface.

	Distance from Fracture		
	3mm	8mm	13mm
Top	204 (670)	197 (641)	202 (660)
Midplane	183 (611)	180 (605)	177 (593)
Bottom	161 (557)	179 (601)	170 (573)

Table 1: Diaphragm cross-sectional Vickers hardness results in HV1 with conversions to tensile strength in MPa in brackets. The tested points are farther from the centre of the diaphragm than the fracture and the measurement locations are approximate. The tensile strength values are estimates based on ASTM A370.

4.4 SEM Inspection

The SEM work was completed to inspect the crack surface for features which would indicate the direction and speed of crack growth, as well any internal features of the sheet metal which may have caused the fracture.

The SEM images show three distinct regions as labelled in figure 4.3: a striated fatigue fracture region, an intergranular fracture region, and a final rubbed fracture region. As the surfaces of the crack remained in contact during and after fracture the beach marks typically associated with fatigue fracture cannot be clearly seen and are assumed to have been worn away, however it appears the crack initiated at the upper surface of the diaphragm and grew approximately a quarter of the way through the sheet. The central region of the fracture surface shows intergranular material failure. This was not expected and indicates weak joining of the grains at the central plane of the material. A possible cause of this weak interface is carbon particulates at the grain boundaries (i.e. between the grains) created by cooling the sheet too slowly after heating for annealing or during some other production step. Figure 4.4 shows one possible particulate.

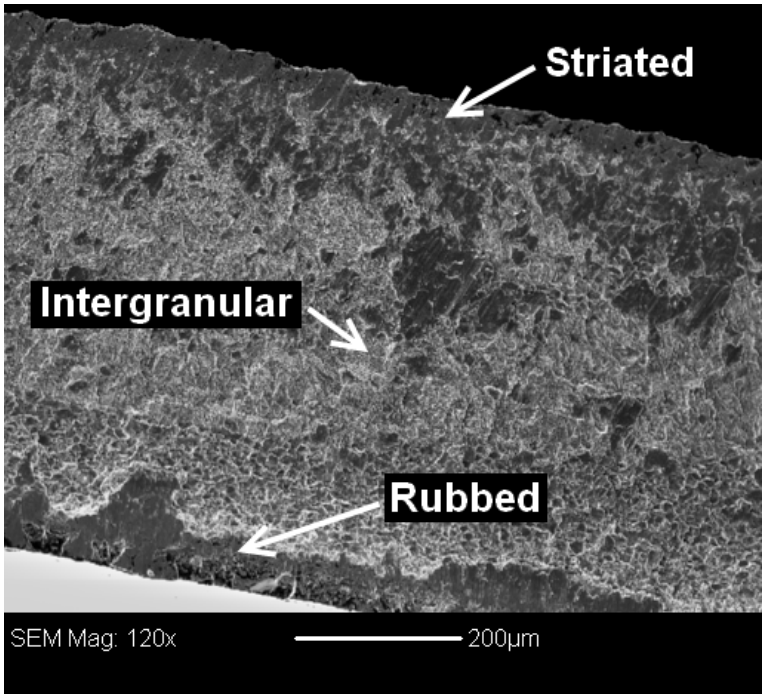

Figure 4.3: SEM image of the fracture surface showing the three surface types as labelled.

The lower region of the fracture surface shows rubbing damage as would be expected as the diaphragm remained in service after fracture. It appears this is the final fracture region as only this area remained in contact after failure.

4.5 Conclusions

It is most likely the crack was initiated at the top surface of the diaphragm and grew down through the material until a through crack developed and became large enough the loss of helium pressure was detected by those operating the PWG.

The material is AISI 430 ferritic stainless steel; however at the central plane of the material there is a region where carbon may have leached from the alloy to form particulates at the grain boundaries. This is detrimental to the integrity of the stainless steel, however as it is at the central plane it is more likely surface condition was the initiating feature which caused the crack. This is supported by the crack's alignment with the brushed surface texture, and reports from IRL that this alignment is both typical, and that no diaphragm without the brushed texture had failed at the time of this test.

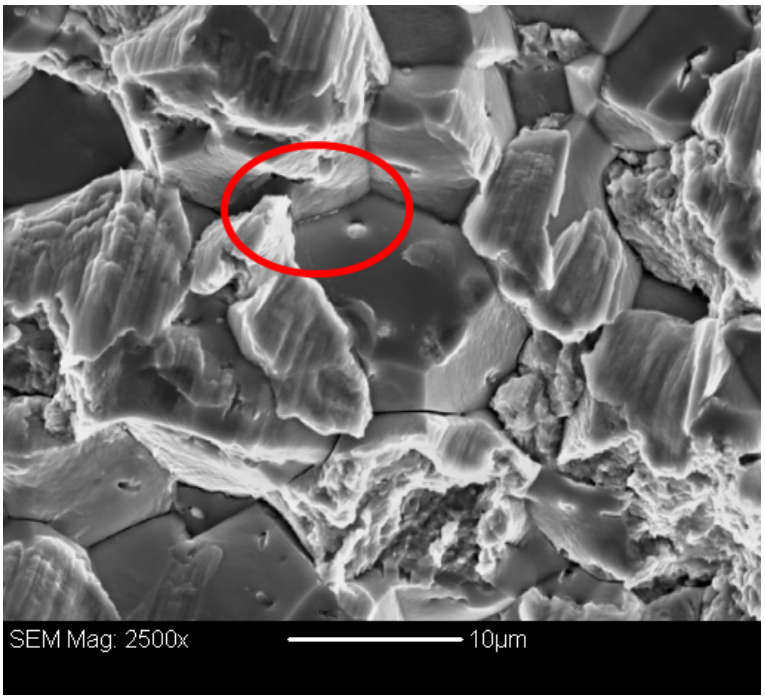

Figure 4.4: SEM image showing possible carbide particulate in the intergranular failure region (circled in red).

Fracture calculations, presented in appendix C, estimate the fatigue life of the component to be very short even for a minute surface defect. These equations were completed using the strains calculated from the supplied SolidWorks FE model, which predicts failure in the cupped region. In section 9 a more thorough FE model suggests a higher stress concentrations exist than those calculated by the SolidWorks FE model, reducing the life expectancy of the component further.

For this type of failure to occur the crack starter needs to be in the high stressed region, and perpendicular to the stress direction. I.e. it must be a circumferential defect at the high stress point. When the diaphragm is manufactured from BA finish stainless steel this type of defect is unlikely and inspection of the component prior to installation could be used to prevent similar failures. For diaphragms manufactured from brushed finish stainless steel this type of defect is much more likely as the brushing creates potential crack starters at all locations, and the circular diaphragm shape causes these potential crack starters to be present in all orientations. It is therefore inadvisable to manufacture diaphragms from brushed metal unless the brush direction is radial at all points on the completed diaphragm.

At the time the fracture analysis was carried out all the diaphragms that had failed had been pressed from brushed AISI 430. This and the fact creating spin forming dies has a shorter lead time has resulted in IRL now fabricating all diaphragms by spin forming bright annealed (BA) AISI 430 sheet. One failure has occurred since, and visual inspection of the failed diaphragm suggests the mechanism is the same as the fracture location is the same, as the diaphragm was sanded after spinning, creating circumferential scratches in the component similar to the brushed texture in the examined component. This reinforces the conclusion that surface condition is highly important in ensuring the survival of the diaphragms, and suggests the stress concentration is a result of the diaphragm shape rather than the fabrication method.

5 Component Fabrication and Materials

5.1 Current Fabrication Methods

IRL has experimented with pressing and spin forming production methods. The diaphragms produced for the original PWG were pressed as this was possible with the equipment available at the time, while more recent components have been fabricated using metal spinning techniques. Diaphragm failures occur in the same way from both manufacturing processes. For this reason the main focus of this thesis is on the diaphragm shape. Details of the forming process are presented here to give a full picture of the component.

5.1.1 Press Forming

Pressed diaphragms are produced by placing a circular flat workpiece in a hydraulic press. The workpiece is clamped in position at the exterior ring and interior flat disk, then the cupped region formed by applying 29 tonnes to the unsupported region via an annular press tool. Once removed from the press the holes in the exterior ring are added with a manual punch tool.

The circularity of the annular press tool cross-section is low, and the press method results in the sides of the cupped region being unsupported by both the die and the press tool during. These features result in the final pressed shape differing from the originally designed shape slightly as the cupped region has conical, rather than wholly toroidal, sides.

Springback has not been accounted for in the die design, however monitoring of the press displacement during pressing revealed the springback to be very small. This is possibly due to the self-supporting shape of the cup. Basic FE models of the process support this hypothesis, however more thorough models cannot be produced without detailed knowledge of the tribological interactions, nor are they necessary.

5.1.2 Metal Spinning

Metal spinning involves clamping the workpiece in a lathe against a formed die. As the workpiece and block are rotated a localised force is applied to the workpiece, pressing is against the die. Starting near the centre of the workpiece the force is slowly moved radially outward, forcing the workpiece material to flow over the block and take on its profile.

Diaphragms produced in this way have a lower failure rate than those produced by pressing. This may be due to the spinning process having a beneficial effect of surface defects by either retexturing the component surface, or creating residual compressive stresses.

IRL presently produces almost all of the PWG diaphragms by metal spinning due to the lower failure rate, easier set up and greater flexibility in altering the component geometry. For example only a new die is required for the production of a new diaphragm radius, as compared to the several interacting components required for a new press tool.

5.2 Material Properties

5.2.1 Presently used Material

The present diaphragms are made from 0.7 mm thick AISI 430 ferritic stainless steel. This material was chosen for its ready availability as a thin sheet, good cold forming performance, and high yield stress. Accepted material properties for this stainless steel are 200 GPa for Young's Modulus, and 0.3 for Possions's Ratio, these can be read from [10]. Additionally the

fatigue strength of the material was shown by Alan Caughley to be between 580 and 450 MPa via accelerated fatigue testing [3].

5.2.2 Potential Alternative Materials

A material with comparable flexibility and a higher fatigue limit would cause any diaphragm design to allow a greater stroke, and produce a greater swept volume. More flexible materials would allow more deformation before the fatigue stress is reached.

The high design life (40000 hours @ 60 Hz) and requirement to reliably contain helium narrows the available materials down to metals with a known fatigue limit. Using the CES Material Selector software developed by M.Ashby the plot shown in figure 5.1 was produced. This scatter plot compares the Young's Modulus and Endurance Limit of metallic materials in the CES library. The optimum material for use as a diaphragm would appear in the lower right corner, i.e. a highly flexible material with a high endurance limit. The black diagonal lines represent AISI 430's ratio of these qualities. The literature values ratio is the line to the left, the measured properties ratio to the right, and the design values the central line.

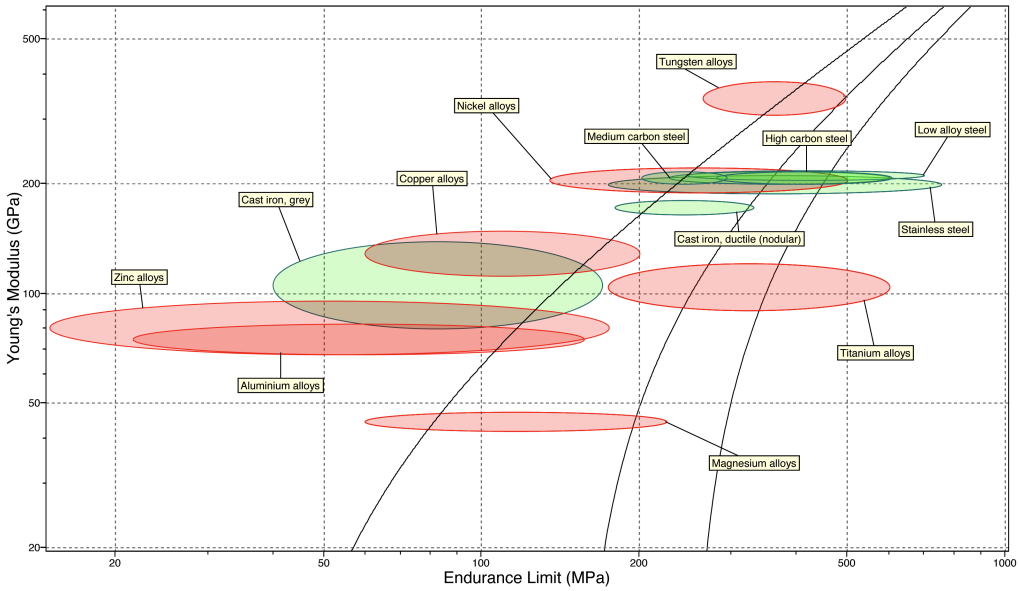

Figure 5.1: Ashby Plot of Potential Diaphragm Materials.

Any material on this plot to the right lower right of the rightmost diagonal line is by the fatigue and flexibility criteria a better material for the diaphragm; factors such as cost, toxicity, reactivity and availability may limit the choice further, however as can be seen from the difference between theoretical and measured values in figure 5.1 materials with comparable theoretical values such as magnesium alloys could also be considered.

From these plots it appears titanium alloys, and many alternative stainless steels could be used to produce a higher performing diaphragm without requiring any change in the currently used shape. Verification of the properties reported in the CES library, as well as in service testing of diaphragms manufactured from these materials would be required before these diaphragms could be used to replace the existing AISI 430 components.

Due to the inconsistencies between the modelled and actual behaviour of the presently used diaphragms it was decided at this point not to continue with the material investigation as a revised diaphragm shape would be applicable to a range of the materials shown, as would be the

shortcomings of the current shape. Assuming any of the potentially better materials shown are suitable for the diaphragm this substitution could equally be made for an alternative diaphragm shape.

6 Finite Element Modelling of Existing Design

6.1 SolidWorks Simulation Model

A model of the existing design was created in SolidWorks during the design of the original PWG. Using this model the sizes of the diaphragm and PWG stroke were determined to maximise the swept volume while ensuring the maximum stress in the diaphragm did not exceed the fatigue strength (including a 28% factor of safety).

As shown in figure 3.2, this model predicts a maximum stress of 381.7 MPa at positive (upward) piston displacement of 1.5 mm. This stress maximum occurs on the interior wall of the unsupported cupped section.

For simplicity the model omits several features:

- The bend radii at all corners including the typical failure point where the cupped section meets the interior disk.
- The central diaphragm indentation. This is not likely to be a critical point from a stress point of view and the effects of changes to this shape on the cupped section are not likely to be significant.
- All detail at a greater radius than the cupped section. This part of the diaphragm cannot move as it is clamped into the PWG frame and so it is modelled without detail and as being unmoveable and perfectly stiff.
- Contact between the piston and diaphragm. The deflection of the diaphragm is introduced to the model as a perfect vertical displacement of the entire central disk.
- Changes in material properties. The entire diaphragm is assumed to have to have the same material properties with no residual stresses, unmodelled stress raisers or differences in material composition as may be present as shown in the SEM images in section 4.

Most of these are unlikely to have a significant effect on the reported stresses. The bend radii and contact conditions do have effects however and these are discussed in section 9. Residual stresses may also have an effect on the diaphragm performance and this is discussed in section 10. The initial ANSYS modelling was done independently and without reference to this model, however once complete this SolidWorks model was used as a reference for the correctness of the final results.

6.2 ANSYS Mechanical Model

The initial ANSYS model was created in ANSYS Mechanical using command line scripts. Scripting was chosen as it gave a high level of control over the material definitions and FE types and could be reviewed quickly without needing a copy of the ANSYS software. Scripting also allowed less specific designs to be trialled by setting ranges for many of the variables and having the software run through all possible combinations.

The initial ANSYS models were created with little reference to the SolidWorks model or to the existing design. This was done to ensure the model was developed independently so errors of technique or approach in the original model were not carried through to the newer model.

The model created is an axisymmetric shell model with 233 elements, as shown in figure6.1.

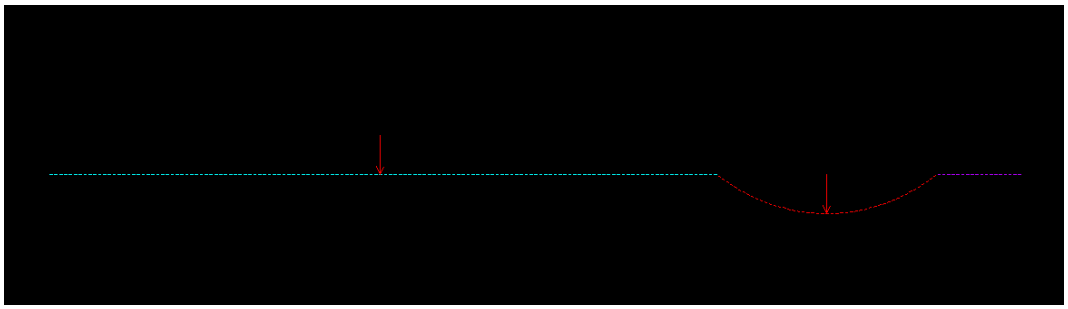

Figure 6.1: ANSYS Mechanical Axisymmetric model. This model is axisymmetric about the left end. The red arrows indicate the applied pressure. The flexible, fixed and displaced elements are shown in purple, red and blue respectively.

This model solves in a few seconds on a desktop computer and calculates the von-mises stress distribution for the upper surface of the diaphragm shown in figure 6.2. The same simplifications as used in the SolidWorks model are used, as are the same forces, constraints and material properties. The ANSYS Mechanical model predicts a slightly different stress distribution to the SolidWorks model, however the highest calculated stress is very similar, 375 MPa for the ANSYS Mechanical model as compared to 381.7 MPa calculated by SolidWorks. The highest stressed point is higher in the unsupported region than calculated in the SolidWorks model, and closer to the actual failure location.

This model was deemed acceptable for testing of the alternative shape concepts.

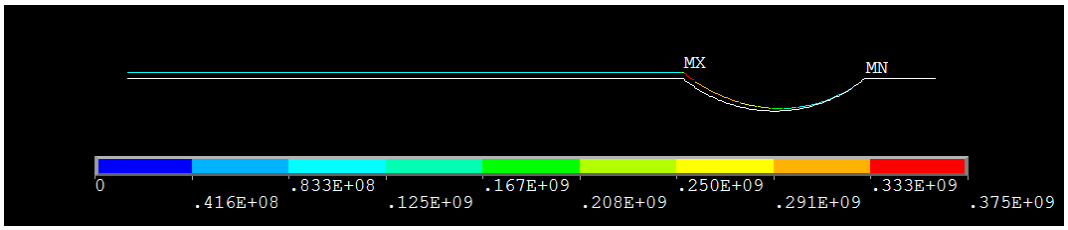

Figure 6.2: Stress distribution in the presently used diaphragm as calculated in ANSYS Workbench. The white line represents the undeformed diaphragm shape. The legend has units of Pa.

6.3 ANSYS Mechanical Optimisation

By modifying the script developed to test the presently used diaphragm dimensions, the dimensions could be optimised. A program could have been produced to find and report these optimum dimensions, instead however the procedure outlined in figure 6.3 was created. This procedure creates a heatmap of the possible dimensions' resulting swept volume capability which can be used decide the most appropriate dimensions. By mapping the results in this way the designer can see not only the most optimum dimensions, but also assess the sensitivity of this and every other set to small changes which may occur during manufacturing.

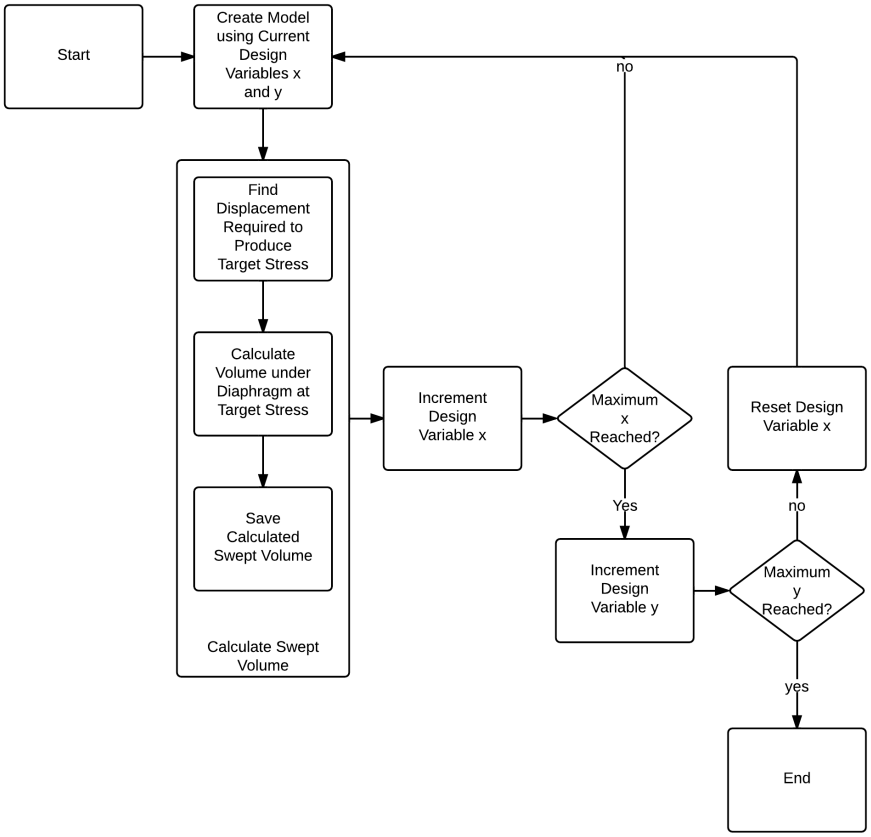

Figure 6.3: Program flow for swept volume heat map creation.

This program can be extended to three or more dimensions, however these are difficult to display in a way that makes the sensitivity and effect of the dimensions clear.

The original script file is attached as appendix D. The program creates the geometry as three regions; the clamped outer ring, the unsupported span, and the piston supported span. The appropriate contact condition is then applied to each region. It is assumed the maximum volume displacement can be found by maximising the piston displacement, so the program finds the critical upward piston displacement which causes the critical stress in the component by bisection, then calculates the volume between the diaphragm and an arbitrary plane. This process then repeats for downward piston displacement and the downward volume is subtracted from the upward volume to give the swept volume.

This process allows non-symmetrical piston displacements but does not allow negative piston displacements. Although it may be possible for an optimum design to exist which requires a continuous positive piston displacement it is expected such a design would have lower swept volume than designs where the stroke is roughly centred about the diaphragm rest position.

6.4 Results and Discussion

From the FE results shown in figure 6.4, the optimum dimensions are 52.5 mm for the unsupported span, and 10.4 mm for the cup depth. This differs from the presently implemented dimensions of 45 mm and 8 mm, which is also marked on the heatmap. A larger copy of the heatmap is included as appendix E.

Bulge Depth as a Proportion of Cup Width

Cup Width (m)	0.1	0.1195	0.139	0.1585	0.178	0.1975	0.217	0.2365	0.256	0.2755	0.295	0.3145	0.334	0.3535	0.373	0.3925	0.412	0.4315	0.451	0.4705	0.49
0.03	-	7.05E-06	3.88E-05	6.35E-05	8.81E-05	1.13E-04	1.41E-04	1.71E-04	1.87E-04	1.89E-04	1.89E-04	1.85E-04	1.82E-04	1.80E-04	1.76E-04	1.75E-04	1.73E-04	1.73E-04	1.73E-04	1.73E-04	1.73E-04
0.0315	-	6.99E-06	4.02E-05	6.99E-05	9.78E-05	1.26E-04	1.61E-04	1.94E-04	1.99E-04	1.97E-04	1.94E-04	1.92E-04	1.87E-04	1.85E-04	1.82E-04	1.78E-04	1.78E-04	1.78E-04	1.78E-04	1.78E-04	1.80E-04
0.033	-	5.19E-06	4.33E-05	7.44E-05	1.07E-04	1.42E-04	1.84E-04	2.09E-04	2.08E-04	2.04E-04	1.99E-04	1.96E-04	1.92E-04	1.89E-04	1.87E-04	1.85E-04	1.84E-04	1.84E-04	1.84E-04	1.84E-04	1.87E-04
0.0345	-	5.15E-06	4.46E-05	7.89E-05	1.18E-04	1.61E-04	2.13E-04	2.20E-04	2.16E-04	2.11E-04	2.06E-04	1.99E-04	1.97E-04	1.94E-04	1.92E-04	1.90E-04	1.89E-04	1.89E-04	1.90E-04	1.90E-04	1.94E-04
0.036	-	-	4.59E-05	8.67E-05	1.29E-04	1.80E-04	2.28E-04	2.28E-04	2.23E-04	2.16E-04	2.11E-04	2.04E-04	2.01E-04	1.97E-04	1.97E-04	1.96E-04	1.96E-04	1.96E-04	1.97E-04	1.99E-04	2.01E-04
0.0375	-	-	4.72E-05	9.43E-05	1.41E-04	2.05E-04	2.39E-04	2.36E-04	2.27E-04	2.19E-04	2.14E-04	2.09E-04	2.04E-04	2.02E-04	2.02E-04	2.02E-04	2.02E-04	2.02E-04	2.02E-04	2.04E-04	2.09E-04
0.039	-	-	4.84E-05	9.68E-05	1.57E-04	2.33E-04	2.47E-04	2.39E-04	2.30E-04	2.24E-04	2.17E-04	2.12E-04	2.09E-04	2.07E-04	2.05E-04	2.05E-04	2.07E-04	2.07E-04	2.07E-04	2.12E-04	2.14E-04
0.0405	-	-	4.96E-05	1.06E-04	1.72E-04	2.61E-04	2.51E-04	2.41E-04	2.35E-04	2.28E-04	2.22E-04	2.15E-04	2.15E-04	2.10E-04	2.10E-04	2.10E-04	2.12E-04	2.12E-04	2.15E-04	2.18E-04	2.20E-04
0.042	-	-	4.91E-05	1.08E-04	1.90E-04	2.67E-04	2.57E-04	2.46E-04	2.37E-04	2.29E-04	2.24E-04	2.19E-04	2.18E-04	2.15E-04	2.15E-04	2.15E-04	2.18E-04	2.20E-04	2.20E-04	2.23E-04	2.26E-04
0.0435	-	-	4.86E-05	1.17E-04	2.08E-04	2.72E-04	2.59E-04	2.47E-04	2.40E-04	2.34E-04	2.27E-04	2.24E-04	2.22E-04	2.19E-04	2.17E-04	2.21E-04	2.24E-04	2.24E-04	2.24E-04	2.30E-04	2.30E-04
0.045	-	-	4.82E-05	1.25E-04	2.37E-04	2.76E-04	2.63E-04	2.51E-04	2.44E-04	2.38E-04	2.31E-04	2.27E-04	2.25E-04	2.25E-04	2.25E-04	2.25E-04	2.27E-04	2.28E-04	2.31E-04	2.33E-04	2.38E-04
0.0465	-	-	4.77E-05	1.34E-04	2.67E-04	2.80E-04	2.64E-04	2.53E-04	2.45E-04	2.39E-04	2.36E-04	2.29E-04	2.29E-04	2.29E-04	2.29E-04	2.29E-04	2.31E-04	2.36E-04	2.36E-04	2.36E-04	2.42E-04
0.048	-	-	4.41E-05	1.39E-04	2.83E-04	2.81E-04	2.68E-04	2.55E-04	2.49E-04	2.43E-04	2.37E-04	2.33E-04	2.33E-04	2.33E-04	2.33E-04	2.33E-04	2.37E-04	2.38E-04	2.40E-04	2.43E-04	2.44E-04
0.0495	-	-	4.37E-05	1.43E-04	2.87E-04	2.81E-04	2.68E-04	2.59E-04	2.47E-04	2.47E-04	2.41E-04	2.37E-04	2.37E-04	2.37E-04	2.38E-04	2.38E-04	2.41E-04	2.41E-04	2.44E-04	2.47E-04	2.47E-04
0.051	-	-	3.86E-05	1.54E-04	3.03E-04	2.84E-04	2.69E-04	2.60E-04	2.54E-04	2.44E-04	2.44E-04	2.43E-04	2.38E-04	2.38E-04	2.43E-04	2.44E-04	2.44E-04	2.44E-04	2.48E-04	2.51E-04	2.51E-04
0.0525	-	-	-	1.59E-04	3.00E-04	2.85E-04	2.72E-04	2.63E-04	2.54E-04	2.51E-04	2.45E-04	2.45E-04	2.42E-04	2.42E-04	2.45E-04	2.45E-04	2.47E-04	2.48E-04	2.51E-04	2.51E-04	2.51E-04
0.054	-	-	-	1.69E-04	3.03E-04	2.82E-04	2.73E-04	2.61E-04	2.58E-04	2.52E-04	2.49E-04	2.49E-04	2.49E-04	2.49E-04	2.49E-04	2.49E-04	2.49E-04	2.49E-04	2.55E-04	2.55E-04	2.55E-04
0.0555	-	-	-	1.85E-04	3.00E-04	2.85E-04	2.73E-04	2.67E-04	2.58E-04	2.55E-04	2.52E-04	2.49E-04	2.49E-04	2.49E-04	2.49E-04	2.52E-04	2.52E-04	2.55E-04	2.55E-04	2.55E-04	2.55E-04
0.057	-	-	-	2.00E-04	2.97E-04	2.85E-04	2.74E-04	2.65E-04	2.59E-04	2.56E-04	2.53E-04	2.53E-04	2.53E-04	2.53E-04	2.53E-04	2.53E-04	2.53E-04	2.53E-04	2.56E-04	2.59E-04	2.59E-04
0.0585	-	-	-	2.10E-04	2.94E-04	2.83E-04	2.71E-04	2.65E-04	2.62E-04	2.59E-04	2.56E-04	2.56E-04	2.56E-04	2.56E-04	2.56E-04	2.56E-04	2.56E-04	2.56E-04	2.59E-04	2.59E-04	2.59E-04
0.06	-	-	-	1.96E-04	2.97E-04	2.83E-04	2.74E-04	2.68E-04	2.62E-04	2.60E-04	2.57E-04	2.57E-04	2.57E-04	2.57E-04	2.57E-04	2.57E-04	2.57E-04	2.57E-04	2.57E-04	2.60E-04	2.60E-04

Figure 6.4: Heatmap produced by the ANSYS Mechanical optimisation script. The values in the map are the maximum possible swept volume for each dimension set in cubic metres. Higher potential swept volume cells are redder while low capability cells are green. Cells without numbers indicate the possible piston stroke before the diaphragm experiences stress in excess of the fatigue stress is below 0.01 mm. The white cell with black text shows the maximum possible swept volume using the present dimensions and the pink cell with red text indicates the maximum possible swept volume calculated.

From the rapid drop in swept volume capability as depth is decreased it is clear that the optimum dimensions by swept volume are not the best dimensions to use, and that a design with a deeper cup has less chance of failing due to manufacturing tolerances.

The presently used dimensions (highlighted in white in figure 6.4) are calculated to give a displacement of 237 mL, rather than the 200 mL of the actual machine. This is in part due the ability of the script to create an unbalanced piston stroke in order to maximise swept volume. The script calculates a downward stroke amplitude of 1.76 mm, and upward amplitude of 1.2 mm, rather than the balanced ± 1.25 mm stroke implemented in the unmodified standard stroke PWG.

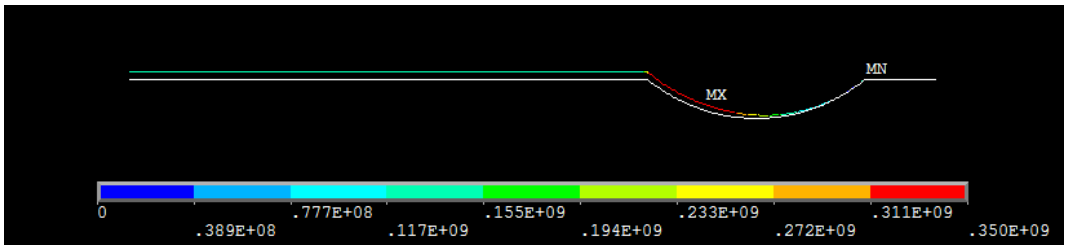

Figure 6.5: Stress distribution at the diaphragm top surface when using the optimal diaphragm dimensions. The units of the legend scale are Pa.

The stress distribution at the optimum dimensions is shown in figure 6.5. The large red area on the inside of the cup indicates that at these dimensions the stress is more evenly distributed across the unsupported diaphragm area. This distributed stress allows the diaphragm to extend further before the stress limit is reached as the average stress is higher.

From this initial optimisation changing the diaphragm dimensions from 45 mm to 54 mm for the span, and from 8 mm to 9.5 mm for the depth as this would result in a 50% increase in swept volume. However it is not advisable to choose dimensions so close to the sudden

drop in swept volume capability that can be seen to the left of the optimum dimensions in the heatmap; a design with a deeper dish but less stroke potential is better as it will require less precise manufacturing tolerances. The main purpose of this optimisation was to create a baseline against which alternative diaphragm shapes could be tested, and to experiment with changing design variables.

The model was run with lower contained pressure, and again with variable material thickness to assess the effects these have on the swept volume. The thickness of the diaphragm was not found to change the swept volume potential significantly, although different material thicknesses required different span and depth dimensions to achieve the same swept volume. The contained pressure was found to have a large effect on the swept volume, with 25% more swept volume being possible at half the contained pressure.

The model was also run with the central disk fixed in the radial direction to investigate the effect of stretching of the central disk across the piston surface on the swept volume. This investigation calculated the swept volume decreases by 3.7% when membrane stresses across the piston surface are prevented. The optimum calculated dimensions are approximately the same as the model which allowed membrane stresses.

7 Concepts for Increasing Piston Stroke

Based on the results of the FE modelling presented in section 6, and suggestions from supervisors and other, the following concepts for maximising the piston stroke were produced.

7.1 Flexible Interface Concepts

7.1.1 Hydraulically Driven Diaphragm

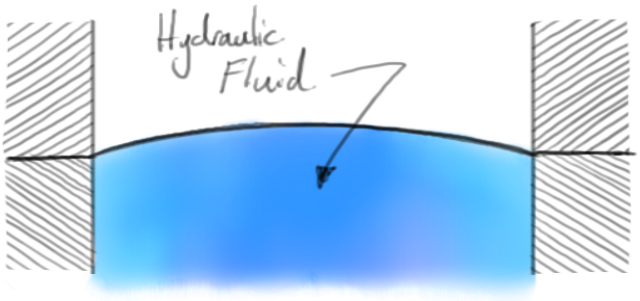

Figure 7.1: Hydraulically Driven Diaphragm Concept Illustration.

By inflating the flexible diaphragm with fluid the diaphragm membrane stress could be shared over a greater diaphragm area. This would take better advantage of the areas currently at well below the fatigue limit and therefore maximise the potential displacement.

This concept was not developed as it is bending stress that creates the most displacement, rather than membrane stresses. Additionally the drive mechanism would either be required to hold the 25 bar helium pressure as well as the differential pressure, or need to be driven by a second diaphragm set that would have similar operating conditions to the current diaphragm.

7.1.2 Stacked Diaphragms

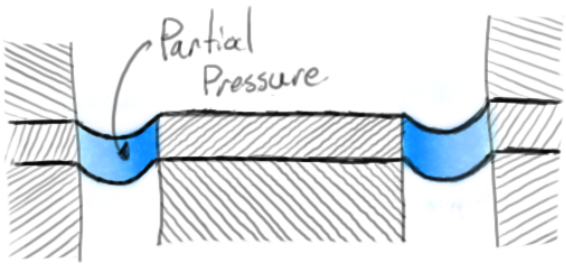

Figure 7.2: Stacked Diaphragms Concept Illustration.

By stacking two or more diaphragms additional pressure vessels would be created between them. This could be used to reduce the pressure difference across each diaphragm allowing a more flexible diaphragm design to be used, resulting in 25% more swept volume when two diaphragms are used, or greater gains with more diaphragms.

This concept was not developed further as it will remain equally applicable for revised diaphragm designs as it is for the currently used geometry. Additionally it will require a more complicated overall PWG design to accommodate the additional sealing requirements, and a more precise commissioning routine that is presently outside what is possible at IRL.

7.1.3 Concentric Diaphragm Supports

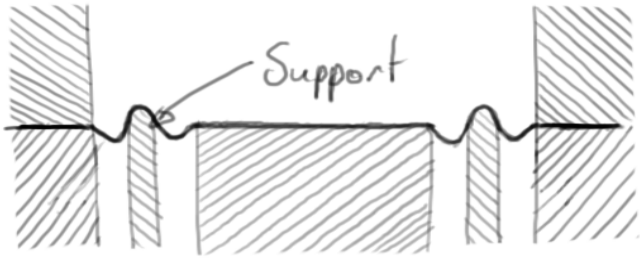

Figure 7.3: Concentric Diaphragm Supports Concept Illustration.

By reducing the unsupported span length the cantilevered forces could be reduced, but the swept volume would also decrease. However by creating several concentric unsupported spans the total swept volume could be increased as the vertical displacement of the interior discs is the sum of their displacement and the displacement of the exterior rings.

Such an arrangement would require a more complicated drive mechanism with concentric pistons of varying strokes, or a support structure similar to those proposed by Brendlin as shown in figure 2.3.

As it is undesirable to introduce additional mechanical complexity to the PWG this concept was not developed further. Additionally the best shape for each concentric unsupported region would likely mimic the shape of what would be optimum for present, single unsupported ring arrangement.

7.2 Diaphragm Shape Concepts

As alternative flexible interface concepts would require an optimised diaphragm shape this is the area of the design the project focussed on. To reduce the number of variables to a manageable level, and to ensure manufacturability of the diaphragm, the thickness and material were kept constant at 0.7 mm and AISI 430.

7.2.1 Circular Corrugations

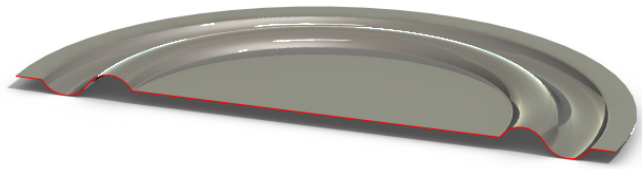

Figure 7.4: Circular Corrugations Diaphragm Shape Concept Illustration. The cut face of this cross-sectional view is highlighted in red.

This is a popular shape for silicon diaphragms of sub centimetre diameter. Because the optimum slope for bending occurs multiple times, and the amount of material available for both bending and membrane stresses is maximised, the potential vertical displacement of the central disk is also maximised.

7.2.2 Rolling Seal

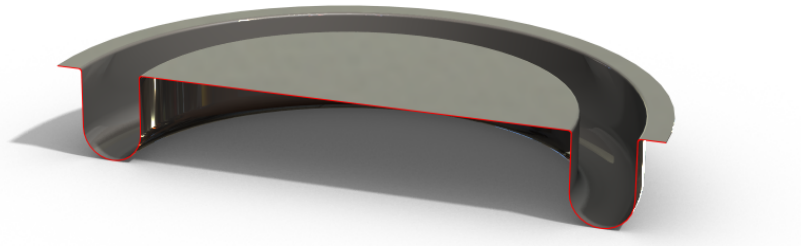

Figure 7.5: Rolling Seal Diaphragm Shape Concept Illustration.

As the piston moves the point at which the diaphragm makes contact moves, trading material between the supported wall and unsupported span. This reduces the amount of extension required from the diaphragm and horizontally supports the side walls, over which membrane stresses can develop. This design also aims to take advantage of the optimum tubular shape for pressure containment.

7.2.3 Conical

Like the corrugated concept, this aims to increase the total material in the unsupported region. Unlike the corrugated concept it aims to increase membrane stresses, and decrease bending stresses, enabling greater swept volume.

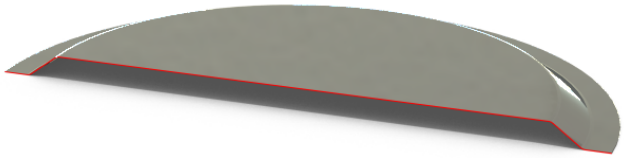

Figure 7.6: Conical Diaphragm Shape Concept Illustration.

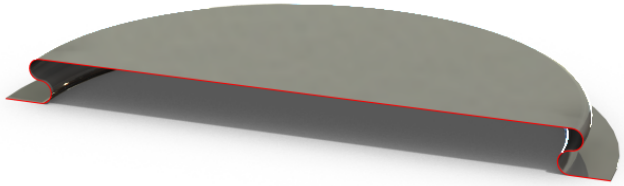

Figure 7.7: Bellows Diaphragm Shape Concept Illustration.

7.2.4 Bellows

Bellows are frequently used situations where flexibility and pressure containment are required. Regardless of their flexibility it will be possible to create a bellows arrangement with a greater swept volume than the current diaphragm design by increasing the overall height. However investigation is required to discover whether this is possible to accomplish the required swept volume in a height that is acceptable.

7.2.5 Balanced Radii

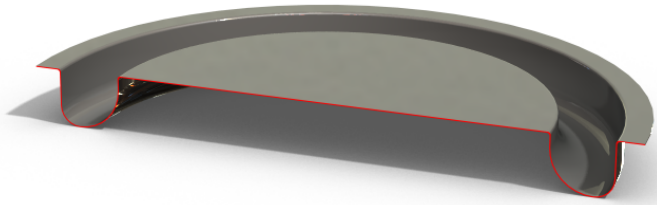

Figure 7.8: Balanced Radii Diaphragm Shape Concept Illustration.

As the diaphragm is axisymmetric the outer side of the unsupported region is larger than the inner side. To balance the horizontal forces created by the pressure on the walls of the unsupported span the radii can be varied to match the horizontal areas. This concept aims to increase the swept volume by increasing the stress on the outer side of the cup to match that of the interior side.

7.2.6 Domed

By allowing the contact point between the diaphragm and piston to move so it is always tangent to both components this concept aims to remove high stress caused by a change in support con-

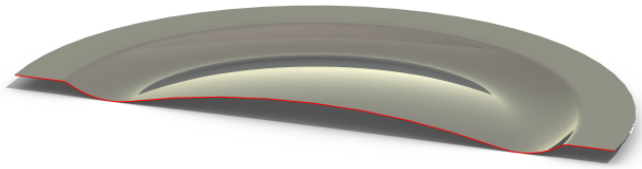

Figure 7.9: Domed Diaphragm Shape Concept Illustration.

ditions. Additionally membrane stresses can develop across the central part of the diaphragm to reduce the stress at the piston edge.

8 Alternative Shape Investigation

Using the same modelling and optimisation technique as was used to find the best dimensions for the presently used shape, several of the concept shapes were trialled. Due to limitations in the way ANSYS handles the scripts, concepts which required nonlinear contact conditions or more than basic trigonometry were not included. By testing each of the concepts over a range of dimensions the optimised versions of each concept can be compared to assess which is best overall. The results of presently used design dimensions, and the sensitivity of the design as assessed from the optimisation presented in section 6 gives a baseline against which the concepts can be compared, showing what concepts should be further developed and what results are unreasonable and should not be relied upon.

8.1 Shape Concept Results

8.1.1 Circular Corrugations

The trials of circular corrugated diaphragms failed to produce any usable geometries as the high flexibility of the profile resulted in large deformations at the corrugation peaks as the pressure and extension work together to flatten the peaks, resulting in large bending stresses. This was not unexpected due to the work of Brendlin presented in section 2.3 being largely focussed on reducing these stresses.

Decreasing the radius of the upward peaks or reducing the overall span of the unsupported region lowers these stresses as less material is available for flattening.

8.1.2 Rolling Seal

As non-linear contact conditions were not available in this simulation this concept did not trade material between the vertical and unsupported regions as envisioned by the concept. As the stresses at the edge of the contact region are low these results imply that this would not occur in a more thorough model either, due to the stiffness of the stainless steel and the high required hoop stresses for rolling to occur.

The performance measured is comparable to, but not as high as, the presently used design with an optimum volume displacement of 250 mL when tested in the same conditions in which the presently used design achieves 272 mL swept volume. This optimum was achieved with an unsupported span of 60 mm. The vertical wall height was shown not to have a large effect on the volume displacement as this only aided by providing a small amount of membrane stress which required high walls in order to have an appreciable effect.

Further trials were performed allowing the unsupported region to be a shallower curve, these resulted in further optimisation however the stroke and volume displacement were not as high as that of the presently used diaphragm as membrane stresses could not develop across the flat central disk.

8.1.3 Conical

This concept performed poorly with optimum volume displacement of 10 mL, approximately 4% that achieved by the presently used design. The optimum was reached with an unsupported span of 8 mm, and a rest height of 6 mm. These results show that although the conical shape on its own is not a suitable replacement, designs with a vertically displaced centre disk at rest are worth exploring.

Based on this finding additional trials of the presently used design were created, but this time varying the height of the central disk. It was found offsetting the central disk by 2 mm could lead to an increase in volume displacement of 3%.

8.1.4 Bellows

To keep the investigation manageable the bellows concept was limited to one complete undulation, with the results assumed scalable to, i.e. the volume displaced could be doubled by doubling the height and number of undulations.

Unfortunately the concept failed in a similar manner to the corrugated profile, with additional support being required if high pressures are to be contained. The trial was modified to allow only one concave corrugation, analogous to the presently used design. This resulted in a required height of approximately 100 mm regardless of the number of corrugations. That is, for a corrugation with a height of 10 mm, ten would be required to match the swept volume of the present design, while for a height of 50 mm only two are required.

8.1.5 Balanced Radii

To simplify the analysis of this concept the form was derived from the rolling seal concept as this allowed the tangent point between the two radii to be calculated without trigonometry, which would otherwise need to be programmed in to the ANSYS script and solved by bisection. As such the results of the rolling seal concept are used for comparison.

Adjusting the ratio of the radii had less effect on the swept volume capability than expected, with the optimum ratio found to be very close to 1:1. Although a small (0.5%) gain in swept volume may be had by varying the radius in this way is was decided not to investigate this concept further.

8.1.6 Domed

As this concept relies on nonlinear contacts it was not explored in using the ANSYS Mechanical script.

8.2 Hybrid Concepts and Discussion

From the above results it is clear diaphragm shapes utilising unsupported corrugations or relying predominantly on membrane stresses are not capable of producing diaphragms that meet the design requirements while being competitive in swept volume with the presently used shape.

The rolling seal concept did not perform as well as hoped as the stiffness of the stainless steel made the rolling action impossible due to high required hoop stresses. This led to performance closely matched to that of the presently used design with a cup depth of half the unsupported span. The balanced radii concept also scored very close to this, showing varying the radius across the span does not have a great effect on the swept volume capability.

The conical results generated show there is some advantage in vertically offsetting the central disk from the clamped outer ring. By combining this concept with the presently used shape the hybrid design illustrated in figure 8.1 was created. This shape increases the diaphragm's unsupported region without reducing the piston radius, resulting in greater flexibility from the unsupported span.

The optimum dimensions for this concept were calculated with a script similar to that shown in appendix D, but with an extra variable dimension added to assess the optimum offset of the

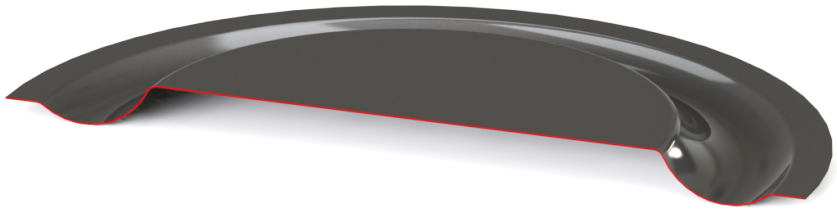

Figure 8.1: Illustration of the vertical offset hybrid diaphragm shape, sectioned along the red surface. This illustrative image has a vertical central disk offset of 15 mm, the calculated optimum vertical offset was is 1.5 mm.

central disk from the clamped outer disk. The optimum calculated dimensions are 56 mm for the span width, 11.2 mm for the span depth (measured from the central disk) and 1.5 mm for the central disk height offset from the clamped outer ring. These dimensions are illustrated in appendix G. The optimum calculated stroke for this diaphragm is +1.6 mm, -2.08 mm, resulting in 9 mL greater swept volume than the presently used shape.

9 Piston-Diaphragm Interface Modelling

9.1 ANSYS Cross-Section and Shell Models

To better understand the contact interactions, FE models of the existing diaphragm were created in ANSYS Workbench. Workbench is a more graphically based front end to the ANSYS FE modelling software engine, and includes optimisation and design investigation tools, as well as a simplified interface for creating nonlinear contacts and a parametric geometry creator which aid in producing models closer to the actual expected operating conditions and component shapes. Unfortunately this software is also limiting in that it is difficult to programmatically access the nodal and elemental data such as that used in the ANSYS Mechanical scripts in section 6 to assess the swept volume.

Two models were created, a shell element based model similar to the original SolidWorks model but more thorough in geometry and contact conditions; and a cross-sectional model, which includes the same constraints and capabilities but solves faster due to it having a smaller number of elements when running at the same spatial resolution as the shell model. Axisymmetric shell models like those used in the earlier analyses are not possible in ANSYS Workbench, nor was it possible to create models which reliably simulate a segment of the diaphragm as if the remainder were there. The ANSYS Workbench models take up to an hour to solve due to a combination of the higher element count and the greater mathematical complexity in solving nonlinear contact problems, making 400 sample investigations as conducted with the ANSYS Workbench models impossible within the time available.

Although the cross-sectional model solves faster than the shell model, the shell model was used extensively as it is better suited to the kind of programmatic optimisation used in section 6, and repeated for more thorough models later in this section.

9.2 Modelling of the Presently Used Shape

The stresses calculated using the cross-sectional model and the shell model are presented in figures 9.1 and 9.2 respectively. The shell and cross-sectional models correlate well, as does the ANSYS Mechanical model (figure 6.2) in the central cup region where the effects of the bend radii are less. The most noticeable difference between the Mechanical model and these Workbench models is the high stress on the interior edge of the interior bend radius. The stress calculated here is approximately 794 MPa in both models, which is well in excess of both the fatigue limit, and the elastic limit of AISI 430.

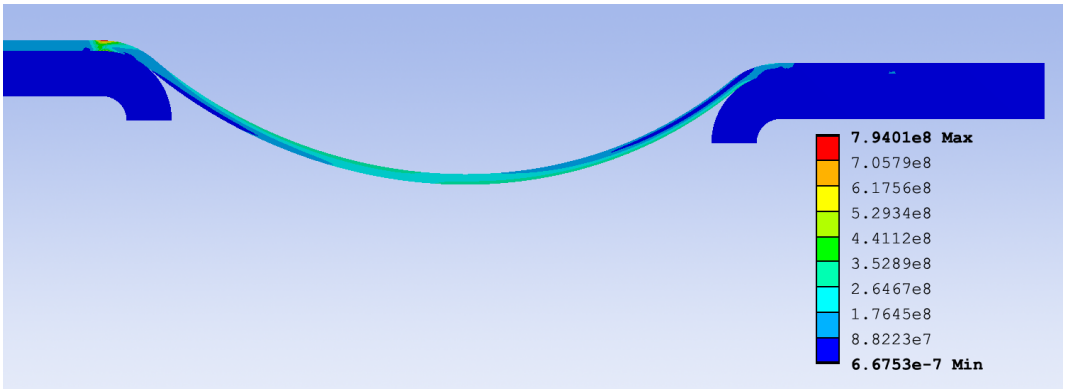

Figure 9.1: Stress Distribution as calculated using an axisymmetric cross-section model in ANSYS Workbench.

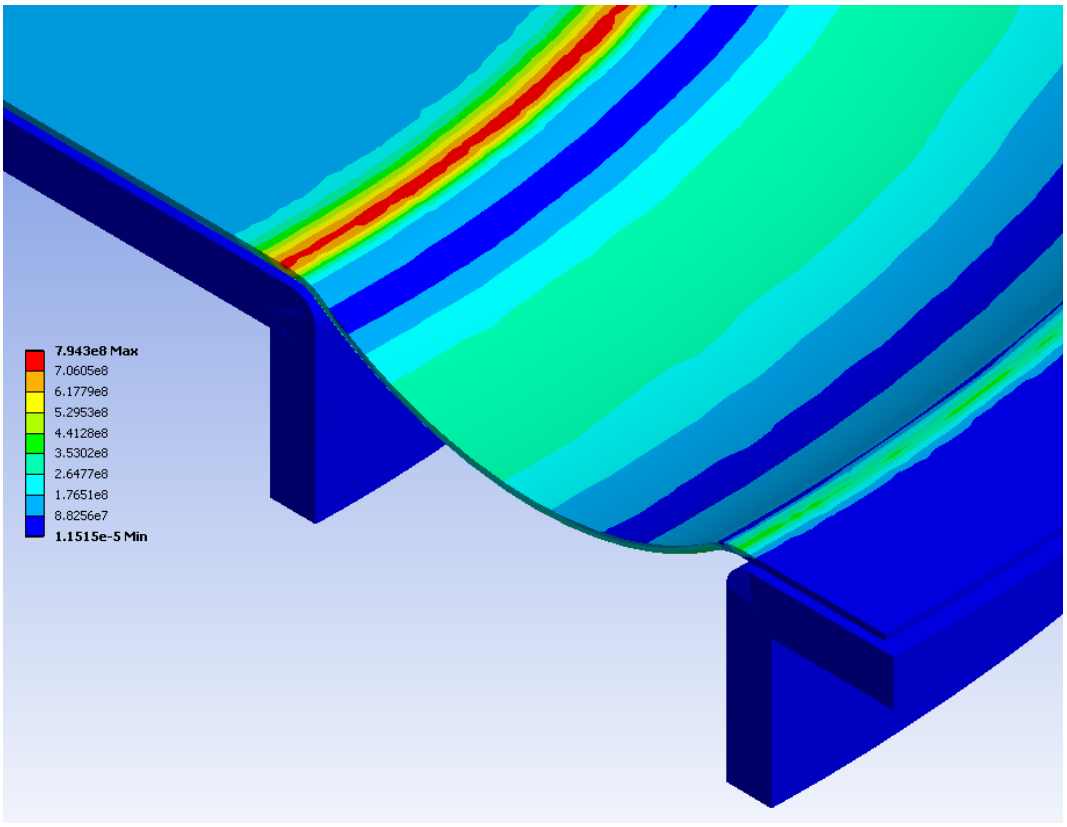

Figure 9.2: Stress Distribution as calculated using a shell model in ANSYS Workbench.

The filleted profile of the piston as can be seen in the ANSYS Workbench models does not match the chamfered profile of the installed piston. This has been done to prevent FE analysis artefacts such as numerical concentrations that otherwise appear due to the sudden change in contact conditions at the piston edge. Such stresses give results similar to the high stress ring observed, however with the stress concentration at the contact edge, on the bottom of the diaphragm.

As the high stress ring is present in all models where unrealistic stress concentrators have been removed, it is thought to be real. In addition to not being at the expected location for a numerical concentration FE artefact the high stress region extends over several elements and does not reduce in size when the element size is reduced. Physical verification of this stress is attempted in section 10, and although the measured stress was not as high as calculated, a concentration is observed.

Reducing this stress, or forcing it to present in a manner less vulnerable to small surface defects, is necessary to create diaphragms with high life expectancy.

9.3 Modelling of Contact Dependent Concepts

The more thorough ANSYS Workbench model was used to gain better understanding of what stresses are present in the diaphragm during operation, and as a baseline against which alternative diaphragm concepts, and modifications to the existing design could be compared.

Concepts tested in the ANSYS Workbench environment due to their dependence on sliding or other inconsistent contact requirements were:

1. **Bellows.** The bellows concept from section 7.2 was retested with sliding contact between

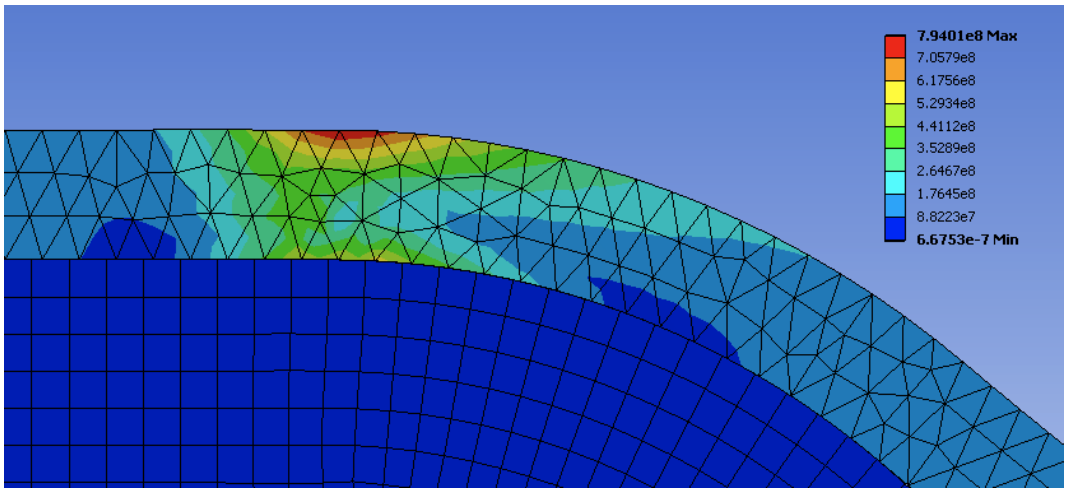

Figure 9.3: Detail of stress concentration showing simulation elements used in the cross-section analysis.

the bellows and the piston or PWG housing walls calculated so that excessive radial deformation of the bellows was prevented.

2. **Rolling Seal.** The rolling seal concept from section 7.2 was retested so the interaction at the edge of the unsupported span could be better understood. As in the bellows concept above the diaphragm is supported by sliding contacts on both the interior (piston) and exterior (PWG frame) sides.

3. **Domed.** The untested domed concept from section 7.2 was tested only with the more thorough model as it requires a variable point of contact between the piston and diaphragm.

Modifications to the existing design tested in the ANSYS Workbench environment were:

1. **Fitted Fillets.** The filleted corners of the diaphragm and piston were made to match, so the stress concentration point was well supported.

2. **Fixing of the Central Disk.** Stretching of the flat central diaphragm disk was prevented so that the filleted edges of the piston and diaphragm centre remained aligned.

The test environment was kept consistent by deriving each of the FE models from the working model of the existing diaphragm and changing the geometry except in the case of the fixed central disk modification where additional constraints were added.

As time and software limitations prevented the kind of optimisation done in section 6, the modifications and alternative geometries were assessed based on their stress performance at ± 1.5 mm piston displacement, with 36 geometry sample points being trialled to hunt for the optimum dimensions. Attempts were made to translate this into more useful volumetric data by simulating intermediate piston displacements and interpolating the results, however the low resolution and high time requirements to gain higher resolution information prevented this from being a useable method of concept analysis.

ANSYS Workbench's built in optimisation was also used, however it proved to be less reliable than required and often suggested geometries which performed worse than what could be produced by reading the optimums from a heatmap.

9.4 Results

In almost all of the concepts tested, stress concentrations were calculated at the points where cross-sectional curves of different radii met. As with the stress concentration calculated in the model of the existing diaphragm these concentrations occur in both the cross-sectional models, and the shell models, suggesting the concentrations are not a simulation artefact, however physical testing is required to verify this.

Ignoring the stress concentrations at the edges of the unsupported span, the bellows supported by the piston or PWG frame would need additional supports at the concave face of the corrugations which are formed into the pressure vessel as high stresses develop due to flattening out of the corrugations by the contained pressure.

The rolling seal concept performed similar to what was predicted by the ANSYS Mechanical model, with the hoop stresses preventing the point of contact between the diaphragm and supporting walls moving vertically. Separation of the diaphragm walls from the supporting walls can occur however, producing small stress concentrations in the diaphragm walls.

Despite not having the small cross-sectional radii the presently used diaphragm design has, which are thought to cause the high fillet stresses, the domed concepts tested have stress concentrations at the edge of the central disk near where the diaphragm and piston separate.

The use of fitted fillets and preventing membrane stresses developing across the central disk moved and reduced the stress concentration as shown in figure 9.5. Preventing membrane stresses across the central disk was required as radial stretching of the central disk otherwise causes the fitted fillets of the piston and diaphragm to become misaligned, allowing bending at the interior edge of the diaphragm where it meets the central disk.

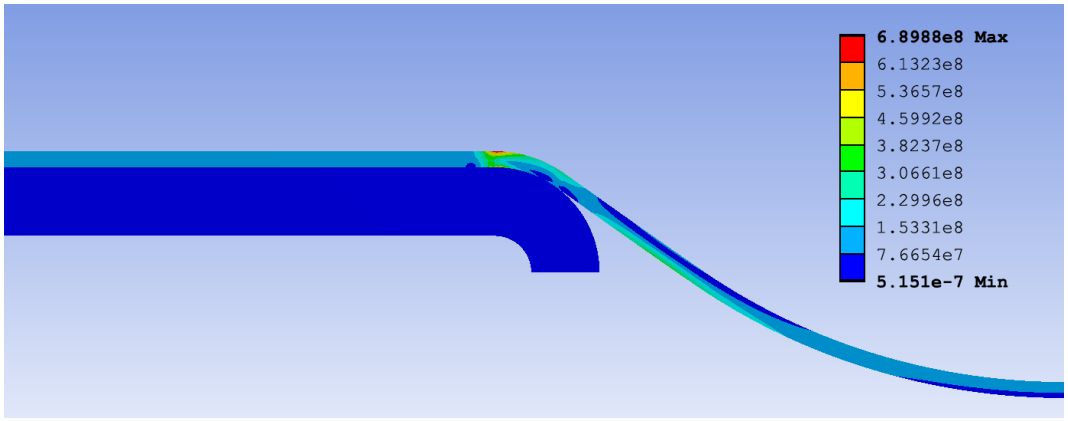

Figure 9.4: Stress distribution calculated at +1.25 mm piston displacement with the central disk free to stretch.

The concentrations are likely due to the difference in stiffness resulting from differing cross-sectional curvature. When two curves of different radii meet there is a sudden change in stiffness analogous to a cantilevered beam which has a step change in thickness. This stiffness change produces a stress raiser at the large cross-sectional radius point furthest from the diaphragm centre as this is the most flexible point. Diaphragm designs that do not have dramatic cross-sectional radii changes may perform better as the stress concentrations may be eliminated, however as shown by the physical testing in section 10 this may not be necessary as points on the diaphragm that are subjected to stresses above the elastic limit of the material may strain harden during commissioning.

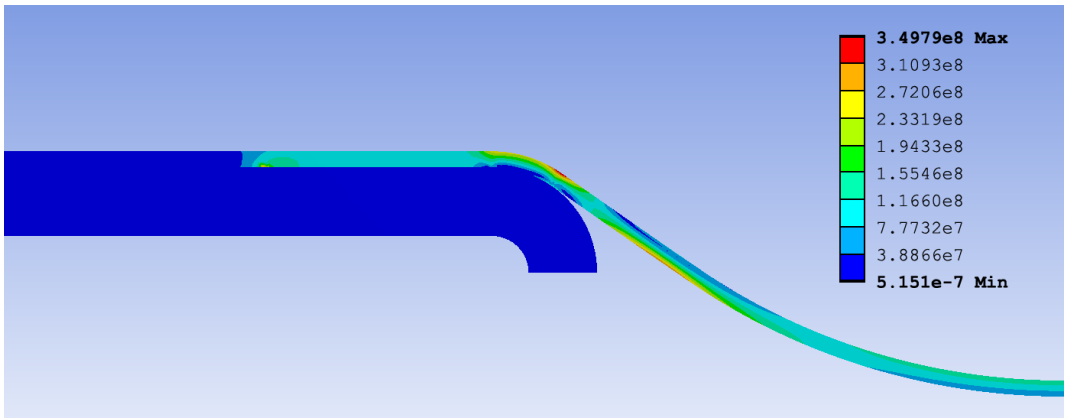

Figure 9.5: Stress distribution calculated at +1.25 mm with the central disk treated as rigid. Note this figure has a different colour scale than figure 9.4 above; the maximum stress calculated is approximately half the maximum stress in figure 9.4.

10 Experimental Verification

To verify the Workbench models a newly pressed diaphragm was mounted in a modified PWG and cycled while the strain was monitored. The major point of interest for this investigation is the stress concentration on the diaphragm's upper surface present in the cross-sectional and shell ANSYS Workbench models. As the strain gauges record strain over a greater area than that of the calculated stress concentration, and that of the finite elements used in the simulations, simulated strain gauges were attached to the FE model for comparison.

10.1 Test Setup

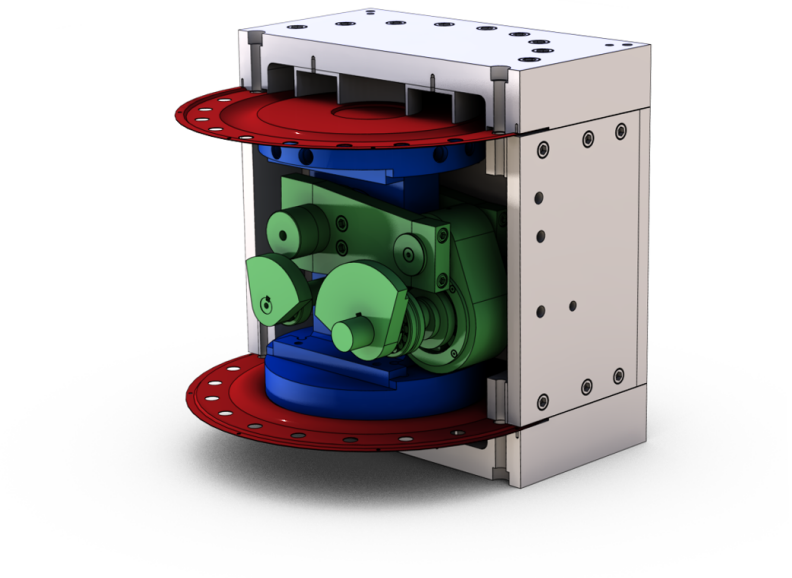

Figure 10.1: Diagram of PWG modified with a second air spring for diaphragm testing.

The PWG used for the verification was modified from that shown in figure 2.2 in several ways:

- The upper portion of the pressure vessel including the pulse tube was removed and replaced with a second gas spring as shown in figure 10.1. Ports to enable cables from inside the vessel to be connected to the instrumentation hardware outside the vessel were drilled in the air spring side wall.

- The electric motor was removed and replaced with a crank so the machine could be driven by hand at a slower rate than the machine would normally run. This way the PWG could be driven slowly enough that dynamic pressure effects would not influence the strain at the diaphragm.

- The upper and lower pressure vessels were connected with copper tubing, creating one vessel with approximately constant volume regardless of the piston position. This was done to ensure the measured strain changes were the result of the piston location, rather than changes in contained pressure.

- The machine was filled with water in the place of helium. This was done to reduce costs, make filling of the vessel easier, and to reduce the dangerous effects leaks would have had the vessel been filled with gas. It also enabled leaks to be seen more easily.

- Strain gauges were attached to the upper face of the top diaphragm as detailed later in this section. The gauges were waterproofed with room temperature vulcanising silicone (RTV) as shown in figure 10.2, and cutouts were made in the gas spring support ring to ensure localised stresses were not caused by the gauges or RTV during commissioning of the PWG. The support ring prevents over extension of the diaphragm during commissioning when the vessel is evacuated.

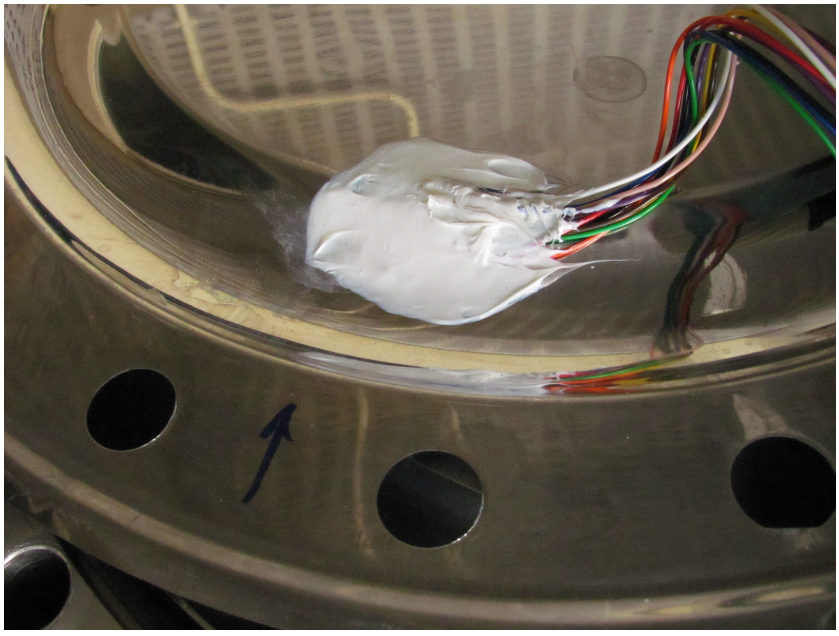

Figure 10.2: Test diaphragm with strain gauges attached and sealed with RTV.

The main feature from the FE models which required investigation was the stress concentration near the edge of the flat central diaphragm disk. The strain gauges were placed so that the first gauge covered this area directly, while the four further gauges were mounted on the upper face of the unsupported span, as shown in figure 10.3. As the calculated stress concentration

is on the upper surface of the diaphragm the gauges were also mounted on the top surface, inside the pressure vessel. This setup was repeated approximately 90 degrees further around the diaphragm circumference so that results from the first set (set A) could be verified against the second (set B).

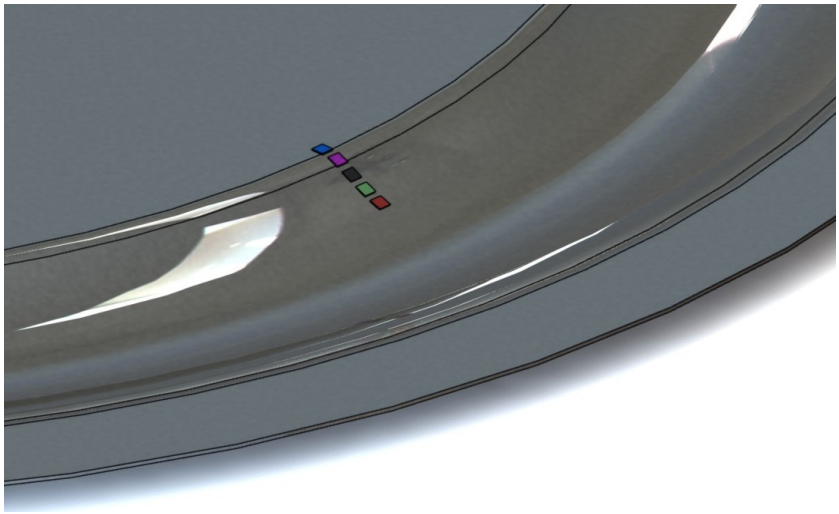

Figure 10.3: Gauge positions on the idealised diaphragm surface showing the "Blue" location as on the flat central disk, the "Purple" location as on the fillet, and the remaining gauges on the diaphragm cup.

The strain gauges used were general purpose foil KFG-2-D9-11 gauges. The strain from these gauges was read using a NI 9219, and logged using a LabVIEW program written specifically for this purpose. As only four channels were available on the NI 9219 at any one time, the ten sensors were split into four groups, and the test run multiple times. The contained water pressure and piston displacement were also monitored, using a Gems 3100 Series compact pressure sensor and Keyence LB-70(W) laser displacement sensor respectively, and logged by the LabVIEW program. The test rig was commissioned by applying a vacuum to the gassprings, then allowing water to be sucked in. Additional water was then pumped in with a hand pump until the relative pressure reached 25 Bar. The output of the strain gauges was logged from before the vacuum was applied so the initial state of the diaphragm could be used as the zero strain reference.

10.2 FEA Emulation of Test Setup

As the area of the strain gauge is larger than the area of the elements used in the FE analysis simulated strain gauges were added to the FE model in the same position and orientation as the actual strain gauges. These gauges were created as a reference lines in the FE model, along which the elastic strains of the underlying elements are reported. The average of the strains of the elements intersecting the reference line is equal to the strain the gauge is expected to experience. As the reference lines cannot be curved, the simulated gauges must be placed slightly below the surface of the modelled component, rather than slightly above as is the case with actual strain gauges. As the curvature of the surface measured increases this could have a significant effect, however at the main point of interest the diaphragm surface is flat, and most of the other gauge locations are on the broad curve of the cupped region. Despite the limitations this way of simulating gauges was found to be more reliable than modelling gauges in the same way one would model a component, then attaching them in the simulated environment. Using reference lines is also faster and easier to implement.

Another possible difference in the simulated strain gauges is positioning. The simulated gauges are placed using much more specific dimensioning than actual strain gauges. To accommodate this the simulated gauges were moved through a range of possible mount positions, producing a strain range within which the strain readings form the actual diaphragm were expected to fall within.

10.3 Experimental Results and Analysis

The expected gauge readings are shown as vertical ranges in figure 10.4; these are reported as ranges which allow for a ± 0.5 mm difference in the gauge mounting position.

In the first test the strain measured at the calculated stress concentration point was higher than the strain at the other gauged positions. Unlike the FE model large strain was also recorded at the black gauge location, 4.5 mm into the unsupported diaphragm span. Additionally the strains at all other gauged locations were lower than those predicted by the model, and in some cases compressive strain was measured, instead of the expected tensile strain.

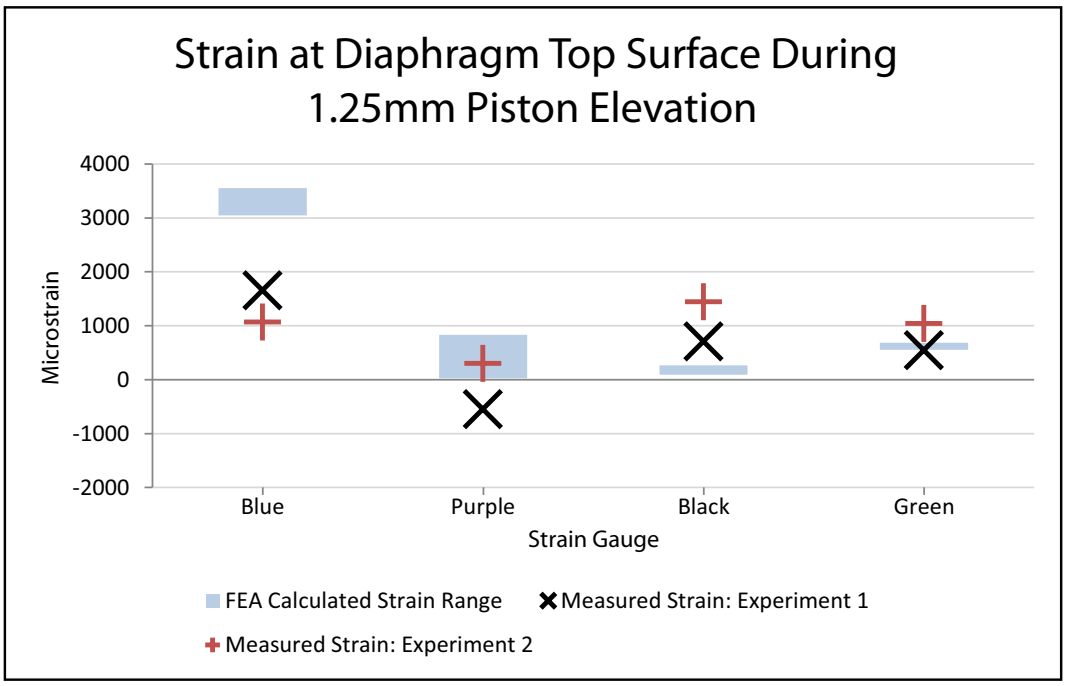

Figure 10.4: Recorded and calculated strain gauge readings. The calculated strain is presented as a range to accommodate probable errors in the gauge mounting position. Similar plots showing the response at the piston rest height, and negative piston displacement are presented in appendix F.

The unexpected black gauge results combined with the large difference between the black strain and that of the neighbouring locations aroused suspicion that the gauges has been compromised by water ingress, which would cause failure of the adhesive as well as potential misreadings due wet gauge contacts. Because of this the original gauges were stripped from the diaphragm and new sets applied.

Retesting the diaphragm with the second set of gauges showed lower tensile strain at the predicted high strain location, and higher tensile strain at the black position, as shown in figure 10.4. Gauge set B showed similar results, however with even lower strain at the blue gauge. Inspection of the diaphragm afterwards showed a small dent in the central disk close to gauge set B, which may account for the higher stiffness (and therefore lower strain) measured at the blue gauge of set B. Similar defects were not found anywhere else on the diaphragm.

10.4 Discussion

As described in section 6, several differences exist between the FE model, and the pressed diaphragm which was used for verification. The modelling simplifications most likely to cause significant differences in the measured strain are the difference in shape, and the lack of residual stresses in the FE model.

The black gauge location is where the diaphragm would be unsupported during pressing. This would cause the diaphragm thickness to be less at this point, as well as the diaphragm shape being conical rather than toroidal as simulated. Both of these would have a negative effect of the stiffness of the diaphragm at this point and so could increase the measured strain.

The predicted and measured stresses at the blue gauge position exceed the elastic limit of AISI 430, meaning plastic deformation will have occurred during commissioning. The low stress measured at the blue gauge of set B in the later runs suggests this introduces advantageous residual stresses in the same way over stroking would.

To thoroughly prove or disprove the stresses as simulated through FE modelling, and to investigate the effect of residual stresses from manufacturing, testing of a diaphragm annealed post manufacture would be beneficial.

11 Conclusions and Future Work

11.1 Tentative Recommendations

From the data collected in this study the following recommendations are made:

- For pressed diaphragms top surface of the stock material should be polished in the region of the interior bend radius and checked for defects so the pressing does not create crack starters. Brushed finish sheet is not appropriate for diaphragm fabrication.
- For pressed and spun diaphragms the upper surface of the interior bend radius must be defect free when the diaphragm is put into service so the high stress predicted by the results in section 9 cannot develop into cracks. Polishing and checking this area is the best way to ensure no stress concentrating defects exist.

If both the above are followed, the diaphragm will be limited by the stress distribution it was originally designed for, as presented in section 3.2. The diaphragm stroke can be increased by:

- Using a diaphragm with an angled unsupported span, so when at rest the flat central disk is not aligned with the exterior clamped disk. Creating an offset between the height of the central disk and the level of the clamped outer ring increases the span of the unsupported region while maintaining a larger piston radius. This results in greater flexibility from the unsupported span. From the investigation in section 8.2 the optimum increase in the height of the central disk is 1.5 mm with a horizontal span of 56 mm. A dimensioned drawing is included as appendix G.
- Moving the centre of the piston stroke so it is not coincident with the height of the diaphragm at rest. The testing in section 6.3 found the maximum upward and downward piston displacements before stresses in the material reached the limit. It was rare for the allowed upward displacement to match the allowed downward displacement. To maximise the swept volume the diaphragm should be taken up to the allowable limit in both directions, so the central height of the piston stroke should not match the rest height of the diaphragm. For the original diaphragm dimensions the calculated stroke capability is +1.2 mm, -1.76 mm. For the suggested diaphragm dimensions (appendix G) the stroke capability is +1.60 mm, -2.08 mm, resulting in 9 mL greater swept volume.

As outlined below, the swept volume of the PWG could be increased by designing for the cyclic stress during pressurised operation, rather than the maximum stress from rest including the stresses caused by the contained pressure. Taking into account the residual stresses in the diaphragm caused by forming may also increase the acceptable stress limits, however as these were not covered in this study no immediate recommendations can be made with respect to these routes for improvement.

11.2 Conclusions

This work intended to optimise the shape of a flexible metal diaphragm for use in low cost cryocoolers. Over the course of the work it became evident that the optimum shape is dependent on the material and fabrication techniques used to create the component. The shape analysis conclusions may not be as quantitatively useful as the finite element solutions suggest, however the analysis of the reasons behind the results remains applicable.

- Greater swept volume performance is possible from a PWG design that does not match the centre of the stroke with the rest height of the metal diaphragm. This is because the stresses distribute differently during positive piston displacement as compared to negative piston displacement but the present diaphragm design has been created assuming the stroke is symmetric. Designing the piston driver to extend to the diaphragm material limit at both ends of the stroke will increase swept volume.
- Greater swept volume is possible from a diaphragm design that with an offset between the clamped outer ring and the central diaphragm disk. This increases the amount of material in the unsupported span without reducing the piston radius.
- Greater swept volume is not possible from the other tested concepts, mainly due to the stiffnesses required to contain the pressure having a negative effect on the flexibility required. Lowering the pressure difference across the diaphragm would allow for greater stroke from the present design and allow other unsupported region profiles to be used.
- The observed diaphragm failures have been caused by the presence of surface defects either during forming or operation. These surface defects either act as crack starters at highly stressed areas of the diaphragm that grow into fractures during operation, or create cracks during fabrication that grow through the component during operation. Polishing the material surface at the critical areas should reduce the probability of this type of failure.
- A high stress concentration exists in the presently used design at the edge of the flat central diaphragm disk. This concentration could act as a crack starter but also may disperse after the PWG is first commissioned as the stress is in excess of the material's elastic deformation limit.
- Residual stresses from fabrication may have a significant effect on the stress distribution in the diaphragm during operation.

11.3 Future Work

- An analysis of the residual stresses in freshly pressed or spun diaphragms, and how further working occurs during commissioning of the PWG could greatly change the assumed limits of the presently used diaphragm design. The changes after fabrication could be assessed by attaching strain gauges and monitoring the strain range changes during operation. This could also be used to assess the effects of overextending the piston during commissioning which may remove both internal and surface stress concentrators.
- Verification of the swept volume gains by off centring of the diaphragm central disk is required before these modifications can be relied upon to improve diaphragm performance. As these small changes have the potential to increase the swept volume without major PWG design changes it is worth exploring.

- Modelling and testing of the diaphragm response as the pressure is varied should allow the negative stroke amplitude to be increased further as the pressure above the diaphragm is less at this piston position. Optimisation of the diaphragm dimensions and piston stroke could be carried out with this in mind once the stress distributions are properly understood.
- An investigation into alternative diaphragm metals such as titanium and high tensile stainless steel will likely find a higher performing material. Testing of these materials and research into their cost and availability is needed before their appropriateness can be assessed.

References

[1] P. Thomas and M. Sheahen, "Cryogenic roadmap," *US Department of Energy Superconductivity Program for Electric Systems*, 2000.

[2] A. Caughley and C. Wang, "Development of a diaphragm pressure wave generator for cryocoolers."

[3] A. Caughley, N. Emery, and N. Glasson, "Diaphragm pressure wave generator developments at industrial research ltd," in *AIP Conference Proceedings*, vol. 1218, p. 695, 2010.

[4] A. Caughley, D. Haywood, and C. Wang, "A low cost pressure wave generator using diaphragms," in *AIP Conference Proceedings*, vol. 985, p. 1122, 2008.

[5] E. Cooke-Yarborough, "Small stirling-cycle power sources in marine applications," in *OCEANS'80*, pp. 457–462, IEEE, 1980.

[6] O. Jeong and S. Yang, "Fabrication and test of a thermopneumatic micropump with a corrugated p+ diaphragm," *Sensors and Actuators A: Physical*, vol. 83, no. 1, pp. 249–255, 2000.

[7] P. Scheeper, W. Olthuis, and P. Bergveld, "The design, fabrication, and testing of corrugated silicon nitride diaphragms," *Microelectromechanical Systems, Journal of*, vol. 3, no. 1, pp. 36–42, 1994.

[8] T. Nguyen, N. Goo, V. Nguyen, Y. Yoo, and S. Park, "Design, fabrication, and experimental characterization of a flap valve ipmc micropump with a flexibly supported diaphragm," *Sensors and Actuators A: Physical*, vol. 141, no. 2, pp. 640–648, 2008.

[9] A. Brendlin, "High pressure membrane," June 11 1940. US Patent 2,203,859.

[10] M. Ashby, "CES material selector 4.5," 2004. Granta Design Limited.

A Adolf Brendlin Patent US2173678

Sept. 19, 1939. A. BRENDLIN 2,173,678

HIGH-PRESSURE BELLOWS STRUCTURE

Filed April 30, 1937 3 Sheets-Sheet 1

Fig. 1

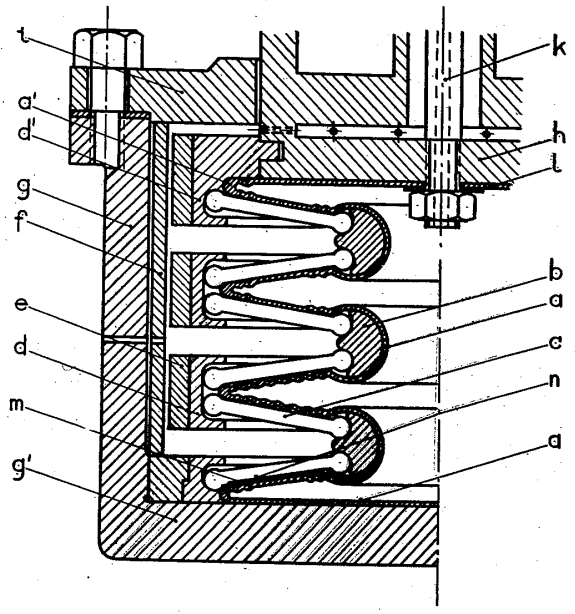

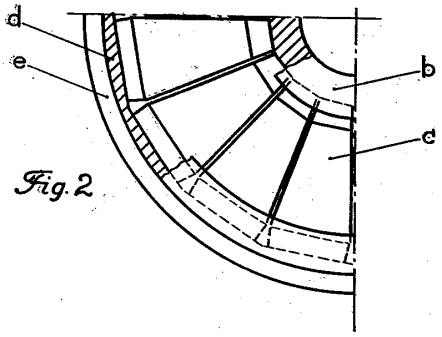

Fig. 2

Adolf Brendlin
INVENTOR

BY Kurtz and Jordan
HIS ATTORNEYS

Sept. 19, 1939. A. BRENDLIN 2,173,678

HIGH-PRESSURE BELLOWS STRUCTURE

Filed April 30, 1937 3 Sheets-Sheet 2

Fig. 3

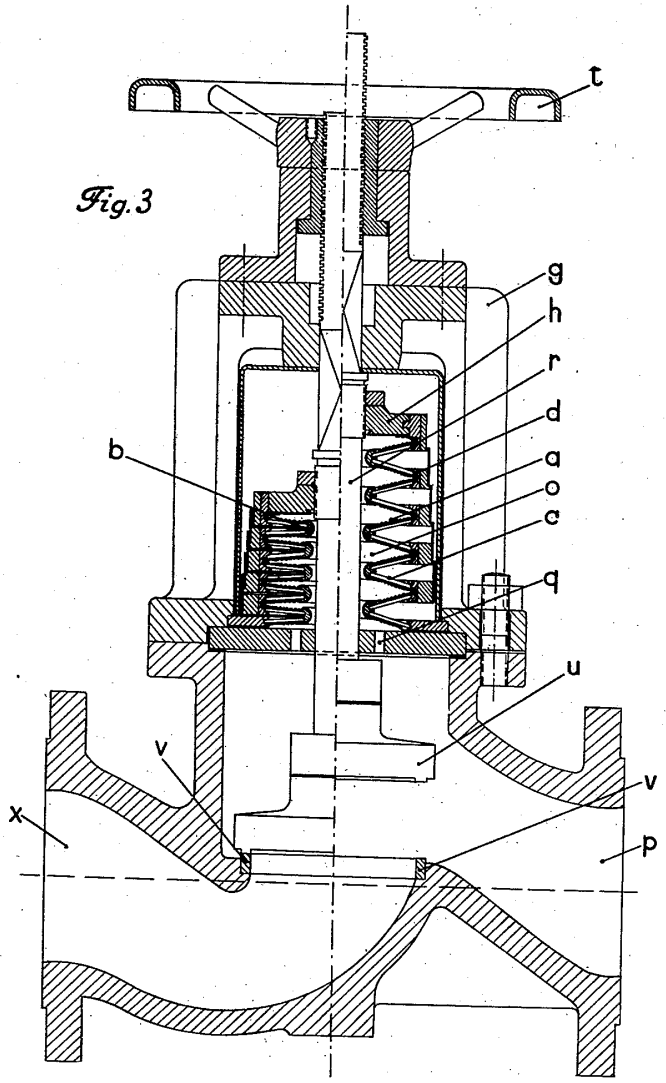

INVENTOR
Adolf Brendlin
BY Hutz and Joslin
HIS ATTORNEYS

Sept. 19, 1939. A. BRENDLIN 2,173,678

HIGH-PRESSURE BELLOWS STRUCTURE

Filed April 30, 1937 3 Sheets-Sheet 3

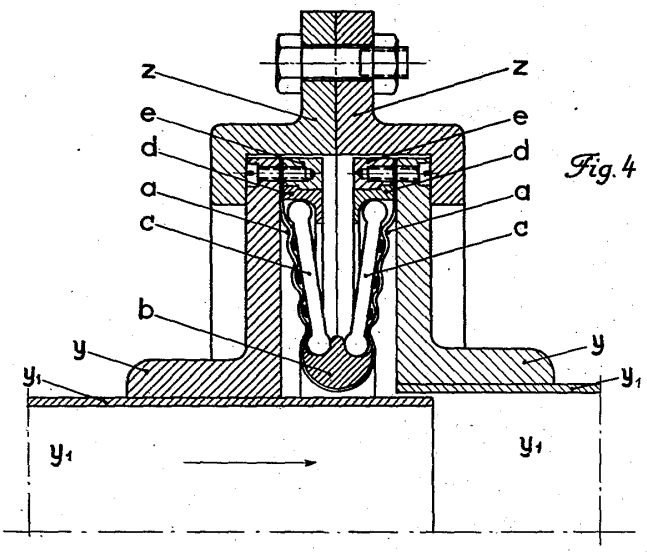

Fig. 4

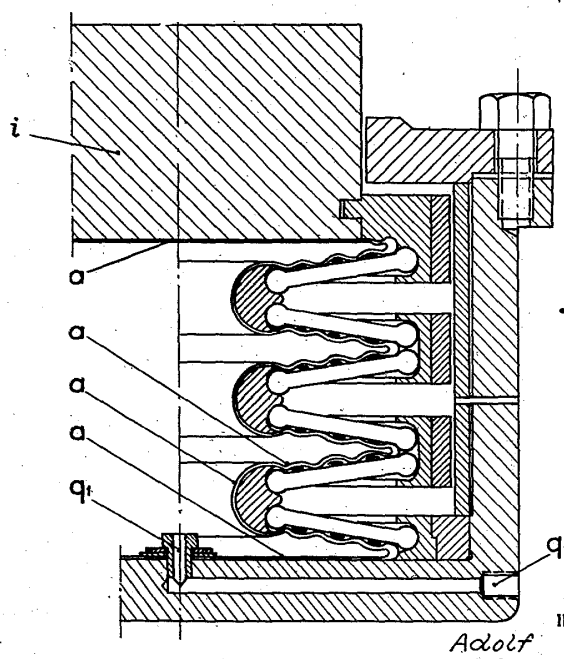

Fig. 5

INVENTOR
Adolf Brendlin
BY Hutz and Joslin
HIS ATTORNEYS

Patented Sept. 19, 1939 2,173,678

UNITED STATES PATENT OFFICE

2,173,678

HIGH-PRESSURE BELLOWS STRUCTURE

Adolf Brendlin, Knapsack, Bezirk, Cologne, Germany

Application April 30, 1937, Serial No. 139,840
In Germany January 10, 1936

11 Claims. (Cl. 137—156.5)

The present invention relates to bellows membranes and bellows membrane bodies for a long stroke and a high pressure.

The membrane and their supports that are used in bellows pumps can be adapted for a long stroke but are suitable only for the transmission of comparatively low pressure. Undulatory diaphragms, namely diaphragms composed of thick-walled box shaped members and longitudinally flexible, are resistant to high pressure but do not permit a long stroke because their flexibility is limited by the thickness of the walls.

High pressure bellows pumps having a long stroke have not hitherto been attainable.

I have found that the bellows membranes and their supports according to this invention are adapted to resist high pressure and when used in a bellows pump, to be capable of a long stroke. They are also suitable for other purposes in which resistance to high pressure and a long stroke are required, for example in constructing membrane pistons, such as high pressure pumps for gases and liquids, pressure pistons for hydraulic presses and lifting arrangements or for gripping any work piece under a high and equal pressure on all sides, but also for any other purposes such as valve gaskets and dashpots in quick closing valves, furthermore, if necessary, in connection with elastic counter-pressure agents, a replacement for air chambers, a safety device for pipe lines and vessels, elastic bodies (compensators) in pipe lines, and for general purposes of tightening, transmitting pressure, elastic suspension or compensating and damping.

The membrane of the present invention is a bellows membrane which consists of a number of membrane discs, seamlessly connected together in series so as to be movable to and from each other; they may be suitably undulated or corrugated. Each of these membrane discs is supported on the face subjected to lower pressure by a number of sector shaped plates mounted in two groups of movable co-axial rings, one group being arranged at the inner ends, the other group being arranged at the outer ends of the sector-shaped plates in such a manner that each ring carries the ends of two adjacent series of supporting plates. The mounting rings of one group may consist of several parts which are held together by a closed ring in order to facilitate dismounting and cleaning.

If the membrane discs are undulated, the supporting plates are preferably correspondingly corrugated. Alternatively, between the membrane discs and the supporting plates there may also be interposed rings whose form corresponds with the undulations of the membrane.

This construction affords a bellows membrane of long stroke and capable of withstanding high pressure without bursting. The two end membranes are secured by further plates or in case of membrane pistons by the wall of the casing or the piston. A membrane piston of this kind has considerable radial play and a long stroke within a guide cylinder (casing) which limits the stroke and renders possible a reciprocal displacement of a pressure fluid and a corresponding device. Furthermore the construction facilitates rapid erection and dismantling of the membrane piston.

As the movable parts which receive the high pressure consist of sector shaped plates arranged in a series and placed with the necessary play in the mounting rings, these plates reciprocally support themselves with the membrane walls, which are also movable, in such a manner that they are relieved from axial pressure. The inner mounting rings are suitably made in one piece while the outer mounting rings consist of several parts for the purpose of easy assembly in the periphery and are held together by external clamping rings; alternatively the outer mounting rings may be in one piece while the inner mounting rings consist of several parts which are held together by a ring. In this construction threaded parts and the like are avoided if possible in order to save space and essentially to simplify the assembly. In this case the membrane serves only for the tightening of the pump chamber. In the case of membrane pistons the piston may be constructed, for instance in such a manner that the completely assembled membrane piston is introduced into the casing (cylinder) and that the end mounting ring is held against the bottom of the casing by the cover of the casing acting through an interposed distance piece.

The stroke may be further elongated by maintaining either the inner or the outer rings variable in their circumference. This may be carried out, for instance in such a manner that the rings are made in several circumferential parts the distance of which is variable from one another and which are held together by springs or holding rings acting as springs. The construction is, however, in this case somewhat more complicated but the stroke may be multiplied. The condition, however, consists in that a membrane of an especially elastic material, for instance of leather, caoutchouc, or of any special artificial substance is used. As during the ex-

pansion of the rings the distance of the ring parts and in these places also of the supporting plates from each other increases, these distances must be bridged over by suitable, movably arranged plates in order to effectively support the membrane.

The operation of the membrane piston may be, for instance, as follows: The pressure fluid is conducted through a pipe, connected with the pressure chamber, into the pressure chamber and the piston rod slides out of the casing until the stroke is complete; the piston stroke may then be reversed by a corresponding reversal of the pressure fluid.

The invention is diagrammatically illustrated by way of example in the accompanying drawings in which

Fig. 1 is half of a longitudinal section through a high pressure membrane piston with its casing;

Fig. 2 is the fourth part of a cross-section through the piston;

Fig. 3 shows the use of a membrane piston for a valve packing; the left hand side of this figure is a longitudinal section of the piston in the closed position and the right hand side in the open position;

Fig. 4 shows the use of a membrane body as an elastic body (compensator) for a high pressure and a long extension power in case of a small total length of high pressure pipings;

Fig. 5 is a membrane piston as pressure piston for a lifting device.

Fig. 1 shows the high pressure membrane piston nearly at the end of its stroke. *a* is the membrane which has a reinforcement at *a'*. The supporting walls for the membrane *a* are the sector shaped plates *c*, the inner mounting rings *b*, the bottom *g'*, of the casing and the wall of the piston head *h*. The outer mounting rings *d* and *d'*, made in several circumferential parts are provided with holdings rings *e*. A reciprocal displacement is avoided by suitable safety devices (not illustrated in the drawings). The control gear of the piston *h* is enclosed in the casing *g*. The piston head *h* is connected with the piston neck. The lowest holding ring is held between the bottom *g'* and the lid *i* by a bushing *f*.

The pressure pipe *k* leading into the pressure chamber is provided with a suitable joint *l* which tightens the membrane *a*.

In order to cover the space between the various sector shaped plates *c* and the transition of the plates *c* to the mounting rings, steel plates *n* or the like and in case of undulated membranes steel rings *m* or the like may be placed below the membrane in order to avoid deformation of the soft membrane material when high pressures are applied or the bearing surfaces of the supporting plates are adapted to the undulated form of the membrane.

In Fig. 3 *a* is the undulated membrane which is supported by supporting plates *c* which are placed in the inner mounting rings *b* and the outer mounting rings *d*. The interior of the membrane piston *o* is connected by canals *q* with that part *p* of the piping which shall be shut off. In the interior of the piston there moves a bar *r* which is rigidly connected with the cover plate *h*; outside of the piston casing *g* this bar is provided with a thread; by rotating the hand wheel *t* on the thread the bar *r* and the cover plate *u* connected with the bar can be lifted or lowered. In the closed position of the valve the plate *u* is strongly pressed against the tightening ring *v* whereby the parts *p* and *x* of the piping are shut off from each other.

The valve thus described is suitable for the shutting off of pipings wherein a high pressure is present and at which pipings ordinary tightening arrangements such as stuffing boxes do not suffice. The movement of the shut off device, in the drawings the plate *u*, may also be performed in any other known manner, but the tightening by the membrane body according to my invention is essential in this case.

In case of the pipe connection by a bellows membrane according to Fig. 4 *y* are the flanges which are rigidly connected with the pipes *y'*. *b* are the inner mounting rings, *d* are the outer mounting rings, *c* are the sector shaped supporting plates and *e* the holding rings, which at the same time press the membrane *a* by means of screws on the flanges *y* and tighten the whole in this place. The distance rings *z* connected with screws give the pipings *y'* the necessary support in an axial or radial direction. These distance rings or the flanges *y* themselves may also be elastically connected with each other whereby the tube pieces are always contracted again.

In Fig. 5 *i'* is the pressure piston of the lifting arrangement, *q'* the connection for the pressure agent and *a* the arrangement of the membrane; the arrangement is the same as shown in Figs. 1 and 2.

I claim:

1. Bellows membrane and bellows membrane body for a high pressure and a long stroke comprising a number of annular membrane discs connected seamlessly in series with each other so as to be capable of moving to and from each other, a number of sector shaped plates by which the membrane discs are supported on the face subject to the lower pressure, and movable mounting rings on both sides of the sector shaped plates in which mounting rings the ends of two adjacent series of supporting plates are flexibly arranged together.

2. Bellows membrane and bellows membrane body for a high pressure and a long stroke comprising a number of annular membrane discs connected seamlessly in series with each other so as to be capable of moving to and from each other, a number of sector shaped plates by which the membrane discs are supported on the face subject to the lower pressure, and two groups of movable mounting rings one group being arranged at the inner ends, the other group being arranged at the outer ends of the sector shaped plates in which mounting rings the ends of two adjacent series of supporting plates are flexibly arranged together, the rings of one group each consisting of several pieces which are held together by a closed ring.

3. Bellows membrane and bellows membrane body for a high pressure and a long stroke comprising a number of annular membrane discs connected seamlessly in series with each other so as to be capable of moving to and from each other, a number of sector shaped plates by which the membrane discs are supported on the face subject to the lower pressure, and two groups of movable mounting rings one group being arranged at the inner ends, the other group being arranged at the outer ends of the sector shaped plates in which mounting rings the ends of two adjacent series of supporting plates are flexibly arranged together, the rings of one group each consisting of several pieces, the distances of which are variable o. each other and which dis-

tances and the distances of the supporting plates in the adjacent places are bridged by movably arranged plates.

4. Bellows membrane and bellows membrane body for a high pressure and a long stroke comprising a number of annular membrane discs connected seamlessly in series with each other so as to be capable of moving to and from each other, a number of sector shaped plates by which the membrane discs are supported on the face subject to the lower pressure, and two groups of movable mounting rings one group being arranged at the inner ends, the other group being arranged at the outer ends of the sector shaped plates in which mounting rings the ends of two adjacent series of supporting plates are flexibly arranged together, the rings of one group each consisting of several pieces, the distances of which are variable from each other and which distances and the distances of the supporting plates in the adjacent places are bridged by movably arranged plates while the pieces are held together by springs or elastic holding rings.

5. Bellows membrane and bellows membrane body for a high pressure and a long stroke comprising a number of annular undulated membrane discs connected seamlessly in series with each other so as to be capable of moving to and from each other, a number of sector shaped plates undulated on the face carrying the membrane discs by which undulated plates the membrane discs are supported on the face subject to the lower pressure, and two groups of movable mounting rings one group being arranged at the inner ends, the other group being arranged at the outer ends of the sector shaped plates in which mounting rings the ends of two adjacent series of supporting plates are flexibly arranged together.

6. Bellows membrane and bellows membrane body for a high pressure and a long stroke comprising a number of annular undulated membrane discs connected seamlessly in series with each other so as to be capable of moving to and from each other, a number of sector shaped plates by which the membrane discs are supported on the face subject to the lower pressure, and two groups of movable mounting rings one group being arranged at the inner ends, the other group being arranged at the outer ends of the sector shaped plates in which mounting rings the ends of two adjacent series of supporting plates are flexibly arranged together and intermediate rings the form of which is adapted to the undulations of the membrane discs and which support the undulations of the membrane discs against the supporting plates.

7. Bellows membrane body for a high pressure and a long stroke comprising a number of annular membrane discs connected seamlessly in series with each other so as to be capable of moving to and from each other, a number of sector shaped plates by which the membrane discs are supported on the face subject to the lower pressure, and two groups of movable mounting rings one group being arranged at the inner ends, the other group being arranged at the outer ends of the sector shaped plates in which mounting rings the ends of two adjacent series of supporting plates are flexibly arranged together, the bellows membrane body being secured on both sides by plates.

8. Bellows membrane body for a high pressure and a long stroke comprising a number of annular membrane discs connected seamlessly in series with each other so as to be capable of moving to and from each other, a number of sector shaped plates by which the membrane discs are supported on the face subject to the lower pressure, and two groups of movable mounting rings one group being arranged at the inner ends, the other group being arranged at the outer ends of the sector shaped plates in which mounting rings the ends of two adjacent series of supporting plates are flexibly arranged together, a casing surrounding the bellows membrane body so as to secure it on the one side while on the other side it is secured by a plate.

9. The use of bellows membrane and bellows membrane bodies for a high pressure and a long stroke comprising a number of annular membrane discs connected seamlessly in series with each other so as to be capable of moving to and from each other, a number of sector shaped plates by which the membrane discs are supported on the face subject to the lower pressure, and two groups of movable mounting rings one group being arranged at the inner ends, the other group being arranged at the outer ends of the sector shaped plates in which mounting rings the ends of two adjacent series of supporting plates are flexibly arranged together for any purposes of transmitting pressure.

10. For use in packing devices bellows membrane and bellows membrane bodies for a high pressure and a long stroke comprising a number of annular membrane discs connected seamlessly in series with each other so as to be capable of moving to and from each other, a number of sector shaped plates by which the membrane discs are supported on the face subject to the lower pressure, and two groups of movable mounting rings one group being arranged at the inner ends, the other group being arranged at the outer ends of the sector shaped plates in which mounting rings the ends of two adjacent series of supporting plates are flexibly arranged together.

11. For use in elastic suspension and dampening devices bellows membrane and bellows membrane bodies for a high pressure and a long stroke comprising a number of annular membrane discs connected seamlessly in series with each other so as to be capable of moving to and from each other, a number of sector shaped plates by which the membrane discs are supported on the face subject to the lower pressure, and two groups of movable mounting rings one group being arranged at the inner ends, the other group being arranged at the outer ends of the sector shaped plates in which mounting rings the ends of two adjacent series of supporting plates are flexibly arranged together.

ADOLF BRENDLIN.

B Adolf Brendlin Patent US2203859

June 11, 1940. A. BRENDLIN 2,203,859

HIGH PRESSURE MEMBRANE

Filed May 26, 1937

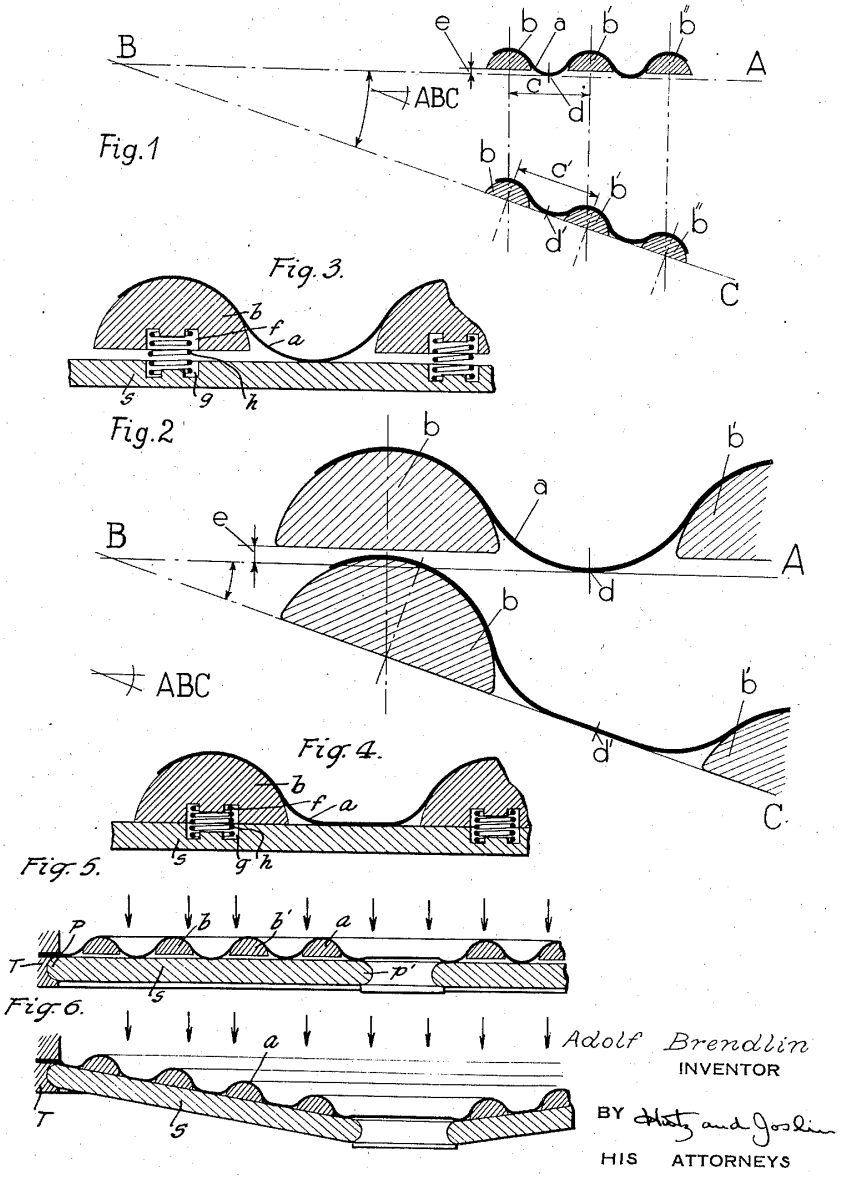

Patented June 11, 1940 2,203,859

UNITED STATES PATENT OFFICE

2,203,859

HIGH PRESSURE MEMBRANE

Adolf Brendlin, Knapsack, Bezirk Cologne, Germany

Application May 26, 1937, Serial No. 144,783
In Germany May 28, 1936

6 Claims. (Cl. 137—157)

The present invention relates to a high-pressure membrane adapted for a very long stroke, that is to say capable of much movement in a direction vertical to its general surface correspondingly with the direction of the pressure.

In order to increase the resistance of membranes in bellows pumps it has been proposed to support the membranes on the face subjected to lower pressure by plates or the like and to provide for a particularly long stroke by a movable arrangement of the supports and by an undulated form of the membrane. It has also been suggested in this connection to mount rings between the supporting plates and the membranes by which the wave crests of the membranes are supported whereas the wave troughs rest on the supporting plates.

I have found that deformation of supported undulated high-pressure membranes as for instance used in the aforesaid bellows pumps, or for similar purposes is avoided still more safely, while the strain on the membranes is reduced and their life is considerably increased, if when the membranes are relieved the supporting means situated between the supports and the wave crexsts of the membranes have a certain play relative to the supports, that is to say if when the membranes are charged the supporting means rest on the supports, while when the membranes are relieved the supporting means are not obliged to be in contact with the plates, but may loosely rest upon them. In this arrangement the wave crests are always carried, in the charged as well as in the relieved membranes, by the supporting means whereas the wave troughs rest on the supports, for instance plates, placed underneath.

The high-pressure membrane of the present invention, therefore, consists of an undulated membrane, essentially flat rigid supports placed underneath this membrane on the face subjected to the lower pressure and supporting means between the supports and the membrane on which means the wave crests of the membrane are carried, the said means resting on said supports when the membranes are charged but having a certain play relative to the membrane or to the support lying underneath them when the membranes are relieved. As supports there may be used plates or the like; the supports need not be quite flat but may be, for instance, slightly curved or corrugated. The supporting means interposed between the supports and the wave crests must correspond with the form of the latter. If the waves are for instance circular, elliptic or of a similar form, this being suitable in many cases, they are supported by corresponding rings whose circumference has the circular or other form of the wave and whose cross section is proportioned in such a manner that the rings fit in the hollow space between the wave crest and the support, for instance a plate, and do not entirely fill this hollow space, but leave a certain play between support and rings. The part of the rings facing the support (plate) is suitably flat so as to rest evenly on the support and at the same time to allow the wave ring a certain relative movement whereby the stroke of the whole device is increased.

Alternatively, the rings may be composed of several flat superimposed single rings; between the single rings there remain spaces which are, however, only present when the membranes are relieved; when charged, the rings are pressed together and against the support. For this purpose the rings are elastically mounted so that when the pressure on to the membrane is released, they may slightly raise the wave crests of the membrane and slightly remove themselves from the support. A slight lateral displacement of the waves and rings is connected with this pressing together, no matter whether these rings consist of one piece or of several superimposed rings. By this arrangement the membrane becomes more movable and admits of a longer stroke.

The entire membrane may have the form of a disk or may be annular or of any other form. The shape of the waves and of the supporting means situated below the wave crests depends on the form of the membrane. An annular, elliptic or similar shape of the membrane and a corresponding construction of the wave crests and the supporting means for the wave crests, is especially suitable for the construction of bellows membranes and bellows pumps wherein the bellows are composed of a number of annular membrane parts of this kind. In any case a high degree of movability of the entire arrangement is attained connected with a resistance to high pressure and furthermore, in each position, a complete relief of pressure on all parts of the membrane by the supporting means placed underneath. As the rather sensitive membrane is relieved of pressure in every way, bellows pumps of this kind are adapted to resist the highest pressure and there does not exist any danger of the membrane leaking.

The invention is diagrammatically illustrated by way of example in the accompanying draw-

ing which represents a portion of a disk-shaped high-pressure membrane tightly clamped or guided at its circumference and corrugated at its center when under pressure.

Fig. 1 is a radial section through this disk, three concentric supporting rings placed one within the other being illustrated together with the membrane in both the relieved and the charged condition of the bellows to which the membrane belongs.

Fig. 2 is a similar view drawn to an enlarged scale.

Fig. 3 is a radial section of a portion of the diaphragm and supporting members in unloaded condition and showing a resilient mounting for the wave crest supporting rings.

Fig. 4 is a view of the same parts but in loaded condition.

Fig. 5 is a radial cross sectional view of the diaphragm and supports in unloaded condition.

Fig. 6 is a similar view in the loaded condition.

The general arrangement of the high pressure membrane in accordance with the present invention at the beginning and the end of the stroke is shown in Figs. 5 and 6 respectively. In the former the diaphragm *a* is shown in unloaded condition suitably clamped or fastened at its periphery in members T. Supporting rings *b*, *b'*, etc., are provided for the wave crests and an inflexible supporting member S which is pivotally mounted at its ends in supports P is arranged opposite the flat sides of the supporting rings *b*. As shown in Fig. 5 the rings *b* are separated from or have a certain play with respect to the supporting member S but in the loaded condition as shown in Fig. 6, the supporting rings rest evenly on the member S.

The undulated membrane *a*, with the supporting rings *b*, *b'*, *b''*, below the wave crests, rests on supporting plates, the smoothly polished surface of which is illustrated by the line A—B. The point B is on the circumference of the membrane where the membrane is clamped or held with freedom to move in a suitable guide. When pressure is applied the surface of the undulated membrane is bulged from A to C so that the angle ABC is formed at B between the original position of the supporting surface A—B and its new position.

When the membrane *a* is relieved from pressure the supporting rings *b*, *b'*, and *b''* have a certain play *e* on the line A—B; in this case the wave crests of the membrane *a* are raised. The wave troughs *d* of the membrane *a* rest, in the relieved state, on the supporting plates.

When the membrane *a* is loaded by the pressure and moved for its stroke, for instance from A to C, the entire extension of the membrane (that is the diameter in the case of a disk) is enlarged or, in other words, the distance of the various supporting rings *b*, *b'* from each other and from the point B becomes greater in the direction B—C than in the direction B—A, while the diameter of the supporting rings *b*, *b'* remains, of course, unaltered. Now the space *e* between the rings *b*, *b'*, *b''* and their support according to the invention proves to be of advantage: By the pressure applied the rings are placed on their support A—C and thus liberate a larger part of the membrane in the wave troughs so that these parts of the membrane extend in the troughs (*d'*) and can thus follow the enlarged distance *b*, *b'* and rest, while being nearly entirely extended, on the support B—C between the rings.

The differing distance between the rings *b*, *b'* from each other are illustrated in the drawing in the unloaded state of the membrane by *c* and in the loaded state by *c'*. Owing to their flat under-surface the rings *b*, *b'* which suitably are elastically mounted in such a manner that they are lifted again from the support A—B when the pressure acting on the membrane ceases, may also slide on the support B—C, in the direction away from B, when pressure is applied and during the movement from A to C. A suitable resilient mounting which permits this movement of the supporting rings *b* is illustrated in Figs. 3 and 4 wherein a recess *f* is provided in the supporting ring *b* and a similar recess *g* is provided in the supporting plate S. A spiral or helical spring *h* is arranged with its ends in the aforesaid recess. The spring *h* lifts the supporting rings *b* from the supporting plates S when the pressure on the diaphragm is relieved. When pressure is applied, however, the springs are compressed into the recess thereby permitting the flat side of the supporting rings to rest evenly on the supporting plates. Also, because of the flexibility of the spring member radial shifting of the supporting rings responsive to the application and relief of pressure on the diaphragms is possible. It will be understood that this showing of the resilient support is intended to be merely illustrative and that many other forms will readily occur to one skilled in this art.

If the rings *b*, *b'* consist of several superimposed, flat single rings, the spaces between these single rings are parallel to the spaces between the rings *b*, *b'*, *b''* and the support A—B illustrated in the drawing. When the rings *b*, *b'* are subdivided into single rings of the kind described, these single rings may be connected with each other like a helix, an elastic support of the wave crests of the membrane being thus afforded.

I claim:

1. A high-pressure membrane which comprises an undulated membrane, rigid, essentially flat supports placed underneath this membrane on the face subjected to lower pressure on which supports the wave troughs of the membrane rest, and means on which the wave crests of the membrane are carried, said means corresponding with the form of the wave crests and resting in the loaded state of the membrane evenly on said supports, in the unloaded state, however, having a certain play relative to the supports in such a manner that when the membrane is charged a deformation of the membrane material is avoided.

2. A high-pressure membrane which comprises an undulated membrane, the waves of which are circular or of a similar form, rigid, essentially flat supports placed underneath this membrane on the face subjected to lower pressure, on which supports the wave troughs of the membrane rest, and rings corresponding with the form of the wave crests of the membrane and carrying these wave crests, said rings in the loaded state of the membrane resting evenly on said supports, in the unloaded state, however, having a certain play relative to the supports in such a manner that when the membrane is charged a deformation of the membrane material is avoided.

3. A high-pressure membrane which comprises an undulated membrane, the waves of which are circular or of a similar form, rigid, essentially flat supports placed underneath this membrane on the face subjected to lower pressure, on which supports the wave troughs of the membrane rest,

and rings corresponding with the form of the wave crests of the membrane and carrying these wave crests, said rings in the loaded state of the membrane resting evenly on said supports, in the unloaded state, however, having a certain play relative to the supports in such a manner that when the membrane is charged a deformation of the membrane material is avoided, each of said rings being composed of several flat superimposed single rings.

4. A high-pressure membrane which comprises an undulated membrane, the waves of which are circular or of a similar form, rigid, essentially flat plates placed underneath this membrane on the face subjected to lower pressure, on which plates the wave troughs of the membrane rest, and elastically mounted rings corresponding with the form of the wave crests of the membrane and carrying these wave crests, said elastically mounted rings in the loaded state of the membrane resting evenly on said plates, in the unloaded state, however, having a certain play relative to the plates in such a manner that when the membrane is charged a deformation of the membrane material is avoided.

5. A high-pressure membrane which comprises an undulated membrane, the waves of which are circular or of a similar form, rigid, essentially flat plates placed underneath this membrane on the face subjected to lower pressure, on which plates the wave troughs of the membrane rest, and elastically mounted rings corresponding with the form of the wave crests of the membrane and carrying these wave crests, said elastically mounted rings in the loaded state of the membrane resting evenly on said plates, in the unloaded state, however, having a certain play relative to the plates in such a manner that when the membrane is charged a deformation of the membrane material is avoided, each of said elastically mounted rings being composed of several flat superimposed single rings.

6. An annular or disk-shaped high-pressure membrane which comprises an undulated membrane, the waves of which are circular or of a similar form, rigid, essentially flat plates placed underneath this membrane on the face subjected to lower pressure, on which plates the wave troughs of the membrane rest, and elastically mounted rings corresponding with the form of the wave crests of the membrane and carrying these wave crests, said elastically mounted rings in the loaded state of the membrane resting evently on said plates, in the unloaded state, however, having a certain play relative to the plates in such a manner that when the membrane is charged a deformation of the membrane material is avoided.

ADOLF BRENDLIN.

C Fracture Equations

Design Properties

The following values have been read from the values calculated by the SolidWorks finite element model created by IRL during the design of the original diaphragm.

Maximum Stress:	352	MPa	σ_{max}
Minimum Stress at Max Stress Point Cycle:	67	MPa	σ_{min}
Mean Stress of Cycle at Point of interest:	209.5	MPa	σ_m
Stress Amplitude:	142.5	MPa	σ_a
Stress at Diaphragm Opposing Face:	85.5	MPa	σ_{opp}
Stress at Diaphragm Midplane:	218.75	MPa	σ_{mp}
Stress Ratio:	0.19	MPa	**R**
Cycle Frequency:	60	Hz	**f**
Operating Duration:	1000	Hours	**h**
Cycles in Life:	2.16E+08	cycles	**N**
Stress Ratio:	0.19	ratio	**R**

Material Properties

These values are from the Granta Design Software suite, supplier specification sheets available on Matweb.com and Mechanical Behaviour of Materials by Norman Dowling. In the cases where Values specific to 430 stainless steel could not be found general values for stainless steels were used.

Fatigue Limit:	237	MPa	σ_f
Poisson's Ratio:	0.275	ratio	**v**
Toughness:	61	$MPam^{0.5}$	K_{Ic}
Walker Equation Constant:	3.24		**m**
Walker Equation Constant:	5.11E-10		C_0
Yield Strength:	205	MPa	σ_o
Stress Life Curve Constant:	1020	MPa	σ'_f
Stress Life Curve Constant:	927	MPa	**A**
Stress Life Curve Constant:	-0.138		**b**

Other Properties

These values are measurements made from the diaphragm or estimates based on the surface finish.

Initial Crack Length:	5.00E-07	m	a_i
Walker Exponent:	0.928		**γ**
Radius at Point of Interest:	0.13	m	**r**
Diaphragm Thickness:	0.0007	m	**t**
Final Crack Length:	0.0007	m	a_f

Stress Based Fatigue Analysis

The number of cycles to failure before fatigue failure occurs can be estimated using the stress based fatigue analysis equation:

$$N_f = \frac{\sigma_a}{\sigma'_f - \sigma_m}^{\frac{1}{b}}{}^{2}$$

Where N_f is the number of cycles. Using the values above this equation gives a component life expectancy of 147753 cycles, which at 60 Hz means the component would survive less than 45 minutes. Setting N_f to the required N of 2.16E8 and solving for σ_a states an acceptable cyclic stress amplitude of 52.13 MPa.

Fracture Mechanics Based Fatigue Analysis

A more specific estimate of the cycles before fatigue fracture occurs can be produced by the fracture mechanics approach, using the crack growth equation:

$$N_f = \frac{a_f^{1-m}{}^{2} - a_i^{1-m}{}^{2}}{C\ F\Delta S\ \overline{\pi}^{\ m}\ 1-m\ 2}$$

Where C is the crack growth constant as calculated with the equation below, F is the finite width factor of 0.728 which refers to the component geometry. ΔS the range amplitude, which was calculated by the SolidWorks FE model to be 108.75 MPa.

$$C = \frac{C_0}{1 - R^{\ m\ 1-\gamma}}$$

Solving the crack growth equation for N_f using the depth of the brushed texture as the initial crack depth a_i gives a component life expectancy of 2647414 cycles, or 12 hours, still well below the desired component life expectancy of 2.16E8 cycles.

Summary

Both fatigue analysis techiniques work on the presumption crack initiation features exist, and both give component life expectancies below one day. To ensure the component can operate indefinitely as required a defect free surface is required.

D ANSYS Mechanical Basic Script

```
/BATCH
! /COM,ANSYS RELEASE 12.1    UP20091102       10:36:32    06/09/2011
!/input,start121,ans,'C:\Program Files\ANSYS Inc\v121\ANSYS\apdl\',,,,,,,,,,,,,,,,1
!*

Testname = 'OriginalUP'

! the range of the variables can be changed here
v1min = 0.1
v1max = 0.49
v1stps = 20
v1inc = (v1max-v1min)/v1stps

v2min = 0.03
v2max = 0.06
v2stps = 20
v2inc = (v2max-v2min)/v2stps

! The direction of displacement is set here, 1 is up, 0 is down
lifts = 1

! Create header in spreadsheet
*cfopen,Testname,csv,,APPEND
*VWRITE,'var1','var2','DI','MaxVMSF','VOLTOTF',
%s, %s, %s, %s, %s
*cfclos

*DO,var1,v1min,v1max,v1inc
    *DO,var2,v2min,v2max,v2inc

        PARSAV          ! Save the parameters so looping works
        /CLEAR          ! Destroy this run's database
        PARRES          ! Read parameters so looping can continue

        ! Settings for run
        SOLV = 1        ! Enables solving of the model,
                        ! disable to stop before the model is solved so manual
                        changes can be made
                        ! If running in a loop (i.e. the optimiser) that will also
                        need to be
                        ! disabled to prevent looping.

        ! General constants and variables
        PI = 3.14159

        ! Define the material limits, and the required accuracy
        MaxMatS = 350000000         ! Max allowed material stress in Pa
        StrsAccu = 0.01             ! Accuracy as a fraction, smaller numbers mean
        the caluclated
                                !  stress is closer to the allowable, but may need
                                more iterations.
        Dead = MaxMatS*StrsAccu     ! Added to the allowed stress to create an upper
        limit, and
                                ! subtracted from the allowed to creat a lower limit.
        Step = 0.001                ! Size of first step in metres. A initial step
        of just under twice
                                !  the actual required displacement will cut down
                                the iterations required
```

```
52
53          ! Define the TDC and BDC Pressures
54          PRBASE = 2500000            ! Base (average) pressure (Pa)
55          PRAMP = 500000          ! Pressure amplitude, i.e. how much the pressure can
            differ by
56          PRTDC = PRBASE+PRAMP        ! Pressure at Top Dead Centre (Pa)
57          PRBDC = PRBASE-0.7071*PRAMP ! Pressure at Bottom Dead Centre (Pa)
58
59          ! Diaphragm geometry.
60          TK = .0007          ! Thickness of the diaphragm material.
61          DPTH = var1*var2    ! Depth of the bulge at it's apex (m)
62          FT = 0.005          ! Fillet Radius (m)
63          OR = 0.1825         ! Radius at the outside of the bulge. (m)
64          IR = OR-var2        ! Radius at the inside of the bulge. (m)
65          OS = 0.1            ! Offset of the model from the ground plane
66          DR = 0.2            ! Radius of the outside of the whole diaphragm. (m)
67          BH2 = OS-DPTH       ! Altitude of the apex of the bulge.
68                          !  The model is raised 100mm so all values are positive.
69
70          BR2 = (IR+OR)/2     ! Radius at the center of the flexible part. (m)
71          BR1 = (IR+BR2)/2
72          BR3 = (BR2+OR)/2
73
74          ! Material Properties.
75          PO = 0.3            ! Poisson's Ratio
76          YM = 200000000000       ! Young's Modulus (Pa)
77
78          ! Check the geometry is valid, the logic here will change for differing shapes
79          ! ok = var2/2 - var1        ! will return positive if the arc length is less
            than 180 degrees
80          ! *IF,ok,LE,0,THEN
81              DIS = 0
82              MaxVMSF = 0
83              VOLTOTF = 0
84          ! *ELSE
85              ! Preprocessor.
86              /PREP7
87
88              NLGEOM,ON           ! Turn large deflection mode on
89
90              ! Draw Profile Points.
91              K,1,0,OS,0,
92              K,2,IR,OS,0,
93              K,3,OR,OS,0,
94              K,4,DR,OS,0
95              K,6,BR2,BH2,0,
96
97              ! Create Interior Disk
98              TOPS = 1
99              L,1,2,
100             TOPE = 1
101
102             ! Create Exterior Disk
103             FIXS = 2
104             L,3,4,
105             FIXE = 2
106
107             ! Create Bulge Crosssection
```

```
BENS = 3
LARC, 2, 3, 6,
BENE = 3

! Material Properties
MPTEMP,,,,,,,,
MPTEMP,1,0
MPDATA,EX,1,,YM
MPDATA,PRXY,1,,PO
ET,1,SHELL209

sect,1,shell,,
secdata,TK,1,0.0,3
secoffset,MID
seccontrol,,,, , , ,

! Mesh lines for analysis
LESIZE,ALL,0.01,,,,1,
LMESH,1,3,

! Fix diaphragm geometries that are not to move
DK,1,UX,0               ! Ensure the centre of the diaphragm is fixed
! Apply fixed constraint to the outer ring
*DO,LNUM,FIXS,FIXE,1
    DL,LNUM,,ALL,0      ! Fix the outer ring
*ENDDO

! Setup the conditions for the situation to be analysed
PR = PRTDC              ! Define the pressure for the point of interest

FINISH

Undr = 1            ! Signifies the target stress has not been exceeded, this
                    !  is used like a firstrun flag in the binary search.
DI = Step           ! Starting displacement in metres, no test is run with this
                    !  displacement and it is assumed it will not be the target.
MaxVMSF = 0         ! Assume stress at zero displacement is zero and that the
                    !  displacement therefore needs to increase.
TooBig = 0          ! Flag for an overstretched diaphragm
TooSml = 0          ! Flag for an understretched diaphragm
NotDone = 1

*DOWHILE,NotDone        ! ,II,1,2           ! For I = 1 to 2:
    ! Binary Search for the displacement that causes the target (i.e. max) stress.
    *IF,Undr,EQ,1,THEN
        Step = Step*2
        DI=Step
    *ELSEIF,MaxVMSF,GT,(MaxMatS+Dead),THEN
        Step=Step/2
        DI=DI-Step
    *ELSE
        Step=Step/2
        DI=DI+Step
```

```
*ENDIF

! Set deformation direction
*IF,lifts,EQ,1,THEN
    DIS = DI
*ELSE
    DIS = -DI
*ENDIF


/PREP7

! Apply Pressure and displacement to the central part of the diaphragm
*DO,LNUM,TOPS,TOPE,1
    DL,LNUM,,UY,DIS
    SFL,LNUM,PRES,PR,
*ENDDO

! Apply pressure to the flexible ring of the diaphragm
*DO,LNUM,BENS,BENE,1
    SFL,LNUM,PRES,PR,
*ENDDO

*IF,SOLV,EQ,1,THEN
    FINISH
    ! Solve
    /SOL
    SOLVE
    FINISH

    ! Post Processing
    /POST1
    PLNSOL,S,EQV,1,10                    ! Plot the displacement and
    vonMises Stress onscreen

    *GET,ELMS,ELEM,0,COUNT               ! Count the elements to be
    stepped through
    VOLTOTF = 0                          ! Create empty total volume
    counter
    *DO,ELM,1,ELMS                       ! Step through every node
        *GET,NODA,ELEM,ELM,NODE,1,       ! Find the node numbers for
        this element
        *GET,NODB,ELEM,ELM,NODE,3,
        *GET,NODC,ELEM,ELM,NODE,2,

        *GET,XOGA,NODE,NODA,LOC,X,       ! Get original x location of
        node A
        *GET,YOGA,NODE,NODA,LOC,Y,       ! Get original y location of
        node A
        *GET,XDIA,NODE,NODA,U,X,         ! Get node X displacement of
        node A
        *GET,YDIA,NODE,NODA,U,Y,         ! Get node Y displacement of
        node A
        XPOSA=XOGA+XDIA                  ! Final x position of node A
        YPOSA=YOGA+YDIA                  ! Final y position of node A

        *GET,XOGB,NODE,NODB,LOC,X,       ! Get original x location of
        node B
```

```
210                     *GET,YOGB,NODE,NODB,LOC,Y,      ! Get original y location of
                        node B
211                     *GET,XDIB,NODE,NODB,U,X,        ! Get node X displacement of
                        node B
212                     *GET,YDIB,NODE,NODB,U,Y,        ! Get node Y displacement of
                        node B
213                     XPOSB=XOGB+XDIB                 ! Final x position of node B
214                     YPOSB=YOGB+YDIB                 ! Final y position of node B
215
216                     *GET,XOGC,NODE,NODC,LOC,X,      ! Get original x location of
                        node C
217                     *GET,YOGC,NODE,NODC,LOC,Y,      ! Get original y location of
                        node C
218                     *GET,XDIC,NODE,NODC,U,X,        ! Get node X displacement of
                        node C
219                     *GET,YDIC,NODE,NODC,U,Y,        ! Get node Y displacement of
                        node C
220                     XPOSC=XOGC+XDIC                 ! Final x position of node C
221                     YPOSC=YOGC+YDIC                 ! Final y position of node C
222
223                     XDIFAB=XPOSB-XPOSA              ! Get the differences
                        between the nodes,
224                     XDIFBC=XPOSC-XPOSB              !  these will be used for
                        calculating areas
225                     YDIFAB=YPOSB-YPOSA
226                     YDIFBC=YPOSC-YPOSB
227
228                     RAAB=XDIFAB*YPOSA               ! Calculate rectangular areas
229                     RABC=XDIFBC*YPOSB
230
231                     TAAB=XDIFAB*YDIFAB/2            ! Calculate trianglar areas
232                     TABC=XDIFBC*YDIFBC/2
233
234                     XCRAAB=(XPOSA+XPOSB)/2          ! Calculate x centroids of
                        rectangular areas
235                     XCRABC=(XPOSB+XPOSC)/2
236                     XCTAAB=XPOSA+2*XDIFAB/3         ! Triangular area centroids
237                     XCTABC=XPOSB+2*XDIFBC/3
238
239                     VORAAB=2*PI*RAAB*XCRAAB         ! Rectangular ring volumes
240                     VORABC=2*PI*RABC*XCRABC
241                     VOTAAB=2*PI*TAAB*XCTAAB         ! Triangular ring volumes
242                     VOTABC=2*PI*TABC*XCTABC
243
244                     VOLELM=VORAAB+VORABC+VOTAAB+VOTABC  ! Total volume for this
                        element
245                     VOLTOTF=VOLTOTF+VOLELM          ! Add this element's
                        contribution to the total volume
246                 *ENDDO
247
248                 NSORT,S,EQV,0,0,  ,0      ! Sort Nodes by von Mises stress.
249                 *GET,MaxVMSF,PLNS,,MAX      ! Store highest stress as MaxVMSF.
250
251                 FINISH              ! Leave Post1
252                 FINISH              ! End this run's everything
253             *ENDIF
254
255             *IF,MaxVMSF,GT,(MaxMatS+Dead),THEN
```

```
256                     TooBig = 1
257                     TooSml = 0
258                     Undr = 0
259                 *ELSEIF,MaxVMSF,LT,(MaxMatS-Dead),THEN
260                     TooBig = 0
261                     TooSml = 1
262                 *ELSE
263                     TooBig = 0
264                     TooSml = 0
265                     NotDone = 0
266                 *ENDIF
267             *ENDDO
268 
269             ! Save screenshot of final result
270             str1 = strcat(chrval(var1),'_')
271             str2 = strcat(str1,chrval(var2))
272             str3 = strcat(Testname,str2)
273             /IMAGE,SAVE,str3,bmp
274         ! *ENDIF
275 
276         ! Write information to .csv file
277         *cfopen,Testname,csv,,APPEND
278         *VWRITE,var1,var2,DIS,MaxVMSF,VOLTOTF,
279 %g, %g, %g, %g, %g
280         *cfclos
281 
282     *ENDDO
283 *ENDDO
284 
```

E Calculated Volume Displacement Heatmap

Bulge Depth as a Proportion of Cup Width

Cup Width (m)	0.1	0.1195	0.139	0.1585	0.178	0.1975	0.217	0.2365	0.256	0.2755	0.295	0.3145	0.334	0.3535	0.373	0.3925	0.412	0.4315	0.451	0.4705	0.49
0.03	-	7.05E-06	3.88E-05	6.35E-05	8.81E-05	1.13E-04	1.41E-04	1.71E-04	1.87E-04	1.89E-04	1.89E-04	1.85E-04	1.82E-04	1.80E-04	1.76E-04	1.75E-04	1.73E-04	1.73E-04	1.73E-04	1.73E-04	1.73E-04
0.0315	-	6.99E-06	4.02E-05	6.99E-05	9.78E-05	1.26E-04	1.61E-04	1.94E-04	1.99E-04	1.97E-04	1.94E-04	1.92E-04	1.87E-04	1.85E-04	1.82E-04	1.78E-04	1.78E-04	1.78E-04	1.78E-04	1.78E-04	1.80E-04
0.033	-	5.19E-06	4.33E-05	7.44E-05	1.07E-04	1.42E-04	1.84E-04	2.09E-04	2.08E-04	2.04E-04	1.99E-04	1.96E-04	1.92E-04	1.89E-04	1.87E-04	1.85E-04	1.84E-04	1.84E-04	1.84E-04	1.84E-04	1.87E-04
0.0345	-	5.15E-06	4.46E-05	7.89E-05	1.18E-04	1.61E-04	2.13E-04	2.20E-04	2.16E-04	2.11E-04	2.06E-04	1.99E-04	1.97E-04	1.94E-04	1.92E-04	1.90E-04	1.89E-04	1.89E-04	1.90E-04	1.90E-04	1.94E-04
0.036	-	-	4.59E-05	8.67E-05	1.29E-04	1.80E-04	2.28E-04	2.28E-04	2.23E-04	2.16E-04	2.11E-04	2.04E-04	2.01E-04	1.97E-04	1.97E-04	1.96E-04	1.96E-04	1.96E-04	1.97E-04	1.99E-04	2.01E-04
0.0375	-	-	4.72E-05	9.43E-05	1.41E-04	2.05E-04	2.39E-04	2.36E-04	2.27E-04	2.19E-04	2.14E-04	2.09E-04	2.04E-04	2.02E-04	2.02E-04	2.02E-04	2.02E-04	2.02E-04	2.02E-04	2.04E-04	2.09E-04
0.039	-	-	4.84E-05	9.68E-05	1.57E-04	2.33E-04	2.47E-04	2.39E-04	2.30E-04	2.24E-04	2.17E-04	2.12E-04	2.09E-04	2.07E-04	2.05E-04	2.05E-04	2.07E-04	2.07E-04	2.07E-04	2.12E-04	2.14E-04
0.0405	-	-	4.96E-05	1.06E-04	1.72E-04	2.61E-04	2.51E-04	2.41E-04	2.35E-04	2.28E-04	2.22E-04	2.15E-04	2.15E-04	2.10E-04	2.10E-04	2.10E-04	2.12E-04	2.12E-04	2.15E-04	2.18E-04	2.20E-04
0.042	-	-	4.91E-05	1.08E-04	1.90E-04	2.67E-04	2.57E-04	2.46E-04	2.37E-04	2.29E-04	2.24E-04	2.19E-04	2.18E-04	2.15E-04	2.15E-04	2.15E-04	2.18E-04	2.20E-04	2.20E-04	2.23E-04	2.26E-04
0.0435	-	-	4.86E-05	1.17E-04	2.08E-04	2.72E-04	2.59E-04	2.47E-04	2.40E-04	2.34E-04	2.27E-04	2.24E-04	2.22E-04	2.19E-04	2.17E-04	2.21E-04	2.24E-04	2.24E-04	2.24E-04	2.30E-04	2.30E-04
0.045	-	-	4.82E-05	1.25E-04	2.37E-04	2.76E-04	2.63E-04	2.51E-04	2.44E-04	2.38E-04	2.31E-04	2.27E-04	2.25E-04	2.25E-04	2.25E-04	2.25E-04	2.27E-04	2.28E-04	2.31E-04	2.33E-04	2.38E-04
0.0465	-	-	4.77E-05	1.34E-04	2.67E-04	2.80E-04	2.64E-04	2.53E-04	2.45E-04	2.39E-04	2.36E-04	2.29E-04	2.29E-04	2.29E-04	2.29E-04	2.29E-04	2.31E-04	2.36E-04	2.36E-04	2.36E-04	2.42E-04
0.048	-	-	4.41E-05	1.39E-04	2.83E-04	2.81E-04	2.68E-04	2.55E-04	2.49E-04	2.43E-04	2.37E-04	2.33E-04	2.33E-04	2.33E-04	2.33E-04	2.33E-04	2.37E-04	2.38E-04	2.40E-04	2.43E-04	2.44E-04
0.0495	-	-	4.37E-05	1.43E-04	2.87E-04	2.81E-04	2.68E-04	2.59E-04	2.47E-04	2.47E-04	2.41E-04	2.37E-04	2.37E-04	2.37E-04	2.38E-04	2.38E-04	2.41E-04	2.41E-04	2.44E-04	2.47E-04	2.47E-04
0.051	-	-	3.86E-05	1.54E-04	3.03E-04	2.84E-04	2.69E-04	2.60E-04	2.54E-04	2.44E-04	2.44E-04	2.43E-04	2.38E-04	2.38E-04	2.43E-04	2.44E-04	2.44E-04	2.44E-04	2.48E-04	2.51E-04	2.51E-04
0.0525	-	-	-	1.59E-04	3.00E-04	2.85E-04	2.72E-04	2.63E-04	2.54E-04	2.51E-04	2.45E-04	2.45E-04	2.42E-04	2.42E-04	2.45E-04	2.45E-04	2.47E-04	2.48E-04	2.51E-04	2.51E-04	2.51E-04
0.054	-	-	-	1.69E-04	3.03E-04	2.82E-04	2.73E-04	2.61E-04	2.58E-04	2.52E-04	2.49E-04	2.49E-04	2.49E-04	2.49E-04	2.49E-04	2.49E-04	2.49E-04	2.49E-04	2.55E-04	2.55E-04	2.55E-04
0.0555	-	-	-	1.85E-04	3.00E-04	2.85E-04	2.73E-04	2.67E-04	2.58E-04	2.55E-04	2.52E-04	2.49E-04	2.49E-04	2.49E-04	2.49E-04	2.49E-04	2.52E-04	2.52E-04	2.55E-04	2.55E-04	2.55E-04
0.057	-	-	-	2.00E-04	2.97E-04	2.85E-04	2.74E-04	2.65E-04	2.59E-04	2.56E-04	2.53E-04	2.53E-04	2.53E-04	2.53E-04	2.53E-04	2.53E-04	2.53E-04	2.53E-04	2.56E-04	2.59E-04	2.59E-04
0.0585	-	-	-	2.10E-04	2.94E-04	2.83E-04	2.71E-04	2.65E-04	2.62E-04	2.59E-04	2.56E-04	2.56E-04	2.56E-04	2.56E-04	2.56E-04	2.56E-04	2.56E-04	2.56E-04	2.59E-04	2.59E-04	2.59E-04
0.06	-	-	-	1.96E-04	2.97E-04	2.83E-04	2.74E-04	2.68E-04	2.62E-04	2.60E-04	2.57E-04	2.57E-04	2.57E-04	2.57E-04	2.57E-04	2.57E-04	2.57E-04	2.57E-04	2.57E-04	2.60E-04	2.60E-04

F Experimental Results

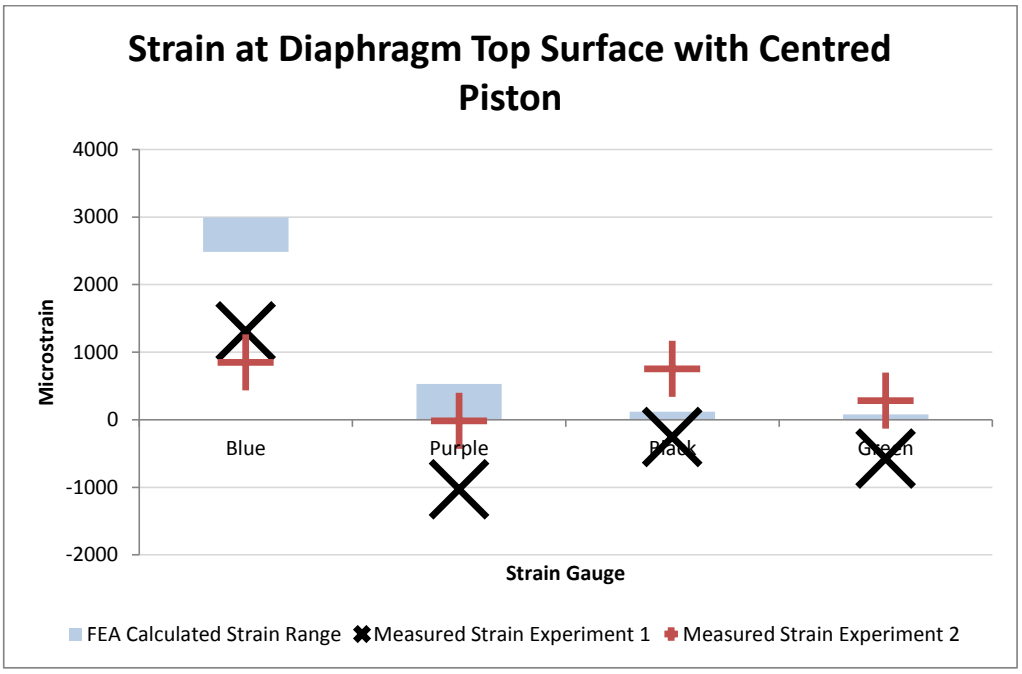

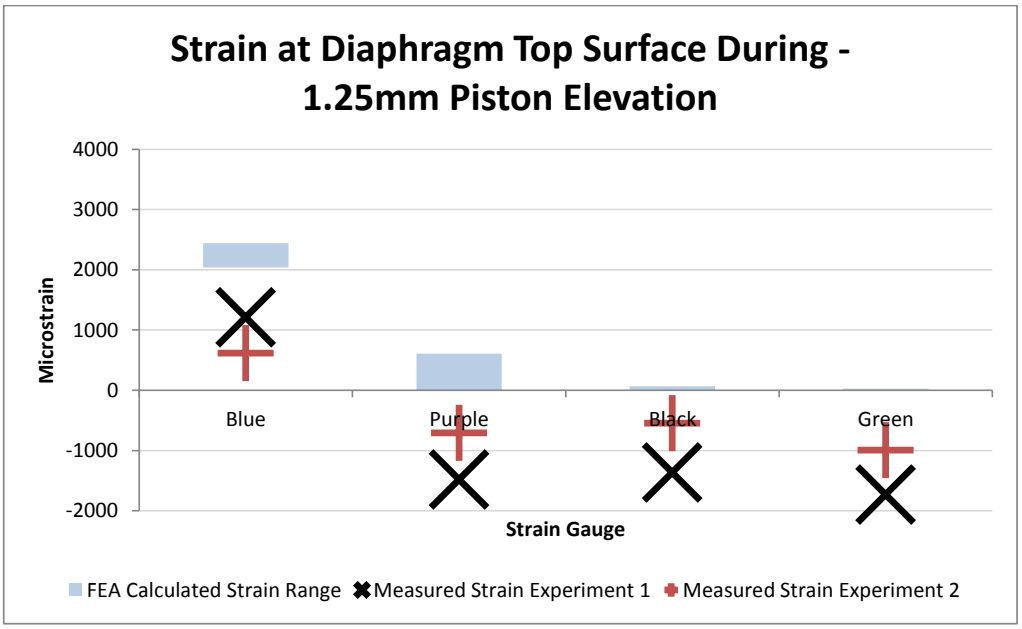

G Suggested Diaphragm Dimensions

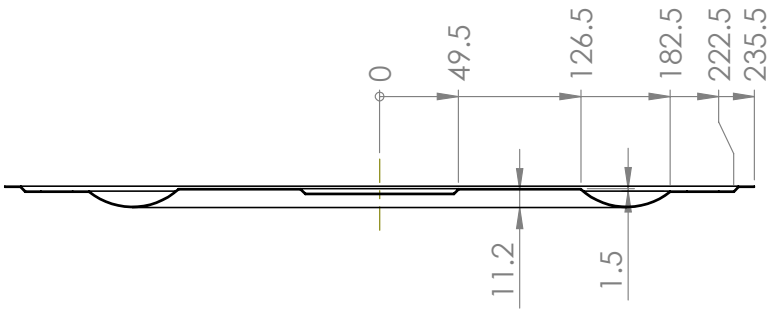

SECTION A-A
SCALE 1 : 4

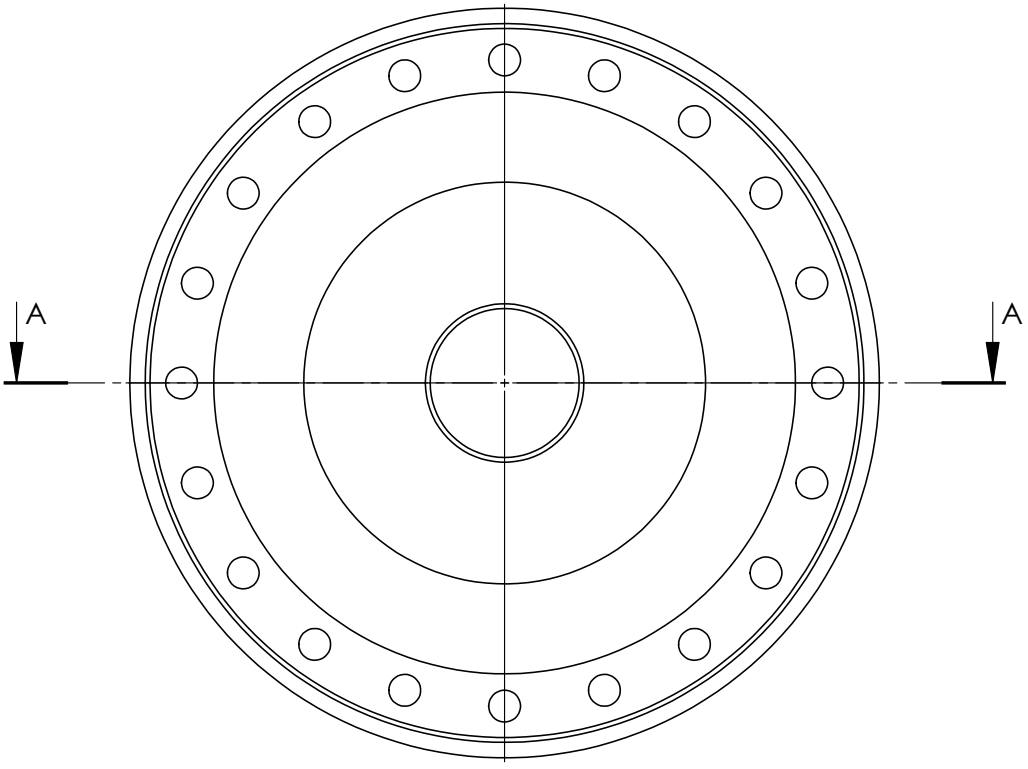

Scale: 1:4
Material: 0.7 mm THK AISI 430 Stainless Steel
All dimensions in millimetres